Supporting Information for

Lysosome-targeted Cyclometalated Ir(III) Complexes as Photosensitizer/Photoredox Catalysis for Cancer Therapy

Yu Chen,[a] *Chao Liang,*[a,] *Manchang Kou,*[b] *Xiaoliang Tang,**[b] *Jiaxi Ru.**[a]

[a] Institute for Advanced Research, Cixi Biomedical Research Institute, Wenzhou Medical University, Zhejiang, 325035, P. R. China

[b] MOE Frontiers Science Center for Rare Isotopes, Key Laboratory of Nonferrous Metal Chemistry and Resources Utilization of Gansu Province, Engineering Research Center of Rare Earth Functional Materials, Ministry of Education, State Key Laboratory of Applied Organic Chemistry, College of Chemistry and Chemical Engineering, Lanzhou University, Lanzhou, 730000, P. R. China

*Corresponding author: E-mail address: rujiaxi@wmu.edu.cn. (Jiaxi Ru) and tangxiaol@lzu.edu.cn. (Xiaoliang Tang)

Contents

Experimental section

Materials and Instrumentation

Materials. All reagents and solvents were obtained commercially and used without further purification unless otherwise noted. DMSO, PBS, Acridine Orange (AO) were purchased from Solarbio (China). 2',7'-dichlorodihydrofluorescein diacetate (DCFH-DA), Lyso-Tracker Green (LTG), Calcein AM (Ca-AM), JC-1 were acquired from Beyotime (China). MitoTracker™ Red FM (MTR) were obtained from Thermo Fisher. Carbonyl cyanide 4-(trifluoromethoxy)phenylhydrazone (FCCP), Nigericin sodium salt and 5-(2,2-dimethyl-1,3-propoxycyclo-phosphoryl)-5-methyl-1-pyrroline N-oxide (CYPMPO) were sourced from MCE (USA). β-NADH, propidium iodide (PI) were bought from aladdin(China). Cytochrome c from bovine, NaN_3 and 5,5-dimethyl-1-pyrroline-N-oxide (DMPO) were sourced from Macklin (China). 2,2,6,6-tetramethylpiperidine (TEMP) were sourced from Bidepharm. Annexin V-FITC/PI kit were bought from Uelandy. Caspase-3/7 activity kit was purchased from Promega (USA). 9,10-Anthracenediyl-bis(methylene)dimalonic acid (ABDA) was purchased from Sigma-Aldrich (USA). $Ru[(bpy)_3]Cl_2$ was obtained from 9dingchem (China). CellTiter 96 AQueous One Solution Cell Proliferation Assay was purchased from Promega (USA). Magic Red MR-$(RR)_2$ was purchased from Immunochemistry Tech (USA). All the compounds tested were dissolved in bio-grade DMSO prior to the experiments.

Caution! Sodium azide (NaN_3) is a highly toxic and potentially explosive substance. It poses significant risks to aquatic life and can have chronic effects. It should be used in minimal quantities to ensure safety.

Measurements. ^1H NMR and ^{13}C NMR spectra were recorded on a JEOL JNM-ECS-400 (400 MHz) spectrometers and referenced to the solvent signals. Mass spectra (ESI) were performed on Bruker Daltonics Esquire6000 mass spectrometers. UV-vis absorption spectra were conducted on a UV-3210PC spectrophotometer. EPR spectra were recorded on a Bruker EMXnano spectrometer. The cell viability assay was recorded using a SpectraMax 190 microplate reader (Molecular Devices). Confocal

images were collected by Leica *Stellaris 5* confocal microscope and analyzed using the Leica Confocal Software. *In vivo* imaging were acquired with an IVIS spectrum (Perkin Elmer).

Phosphorescence quantum yield and lifetimes

The phosphorescence lifetime was determined on an Edinburgh FLS920 time-correlated pulsed singlephoton-counting instrument. Phosphorescence quantum yields at room temperature were measured by the optically dilute method with an aqueous solution of $[Ru(bpy)_3]Cl_2$ (Φ_{em} = 0.028) as the standard solution and by using the equation

$$\Phi_{\mathrm{u}} = \Phi_{\mathrm{s}} \frac{D_u A_s n_u^2}{D_s A_u n_s^2}$$

where Φ is the quantum yield, D is the integrated area of the emission spectrum, A is the absorbance at the excitation wavelength, n is the refractive index of the solution, and the subscripts u and s refer to the unknown and the standard, respectively.

Lipophilicity Measurement

Take the same volume of n-octanol and water (20 mL), in a constant temperature oscillator and shake for 24 h, so that the two phases can be saturated with each other. The mixture was allowed to stand until it naturally separated into two distinct layers. Then, the two-phase distribution is carried out. The **IrL** were added to a mixture of 2 mL water-saturated n-octanol and 2 mL n-octanol saturated water to reach final concentration of 10 μM. The solution was mixed and vibrated in a constant temperature oscillator overnight. After stationary, the two-phase solutions were dispersed, and **IrL** was quantified by the absorbance of the absorption wavelength at 278 nm. The calculation formula is that the concentration of log $P_{o/w}$ = complex in n-octanol phase / the concentration of complex in water phase = c (n-octanol phase) / c (water phase). All the lipophilicity measurements were performed as duplicates of triplicates and the standard deviations (SD) were calculated.

Electron paramagnetic resonance (EPR)

The EPR measurements were carried out with a Bruker EMXnano spectrometer at 298K. The capillary tubes were put into the EPR cavity, and the spectra were recorded

after irradiation at selected times. The spin trapping agent 2,2,6,6-tetramethylpiperidine (TEMP, 1.5 M) was used to detect the $^1O_2$ produced by **IrL** (100 μM, DMSO) in methanol under 390 nm irradiation. 5,5-dimethyl-1-pyrroline-N-oxide (DMPO) was used to verify the formation of OH• in H_2O solutions containing **IrL** (100 μM, DMSO) and DMPO (100 mM) under 390 nm irradiation. The instrument is set as follows: field modulation is 2.0 G, microwave power is 0.32 mW, x-band frequency is about 9.63 GHz, 25 dB microwave attenuation, time constant is 1.28 ms, scanning time is 10 seconds, conversion time is 5 ms.

NAD• radicals were captured by 5-(2,2-dimethyl-1,3-propoxycyclo-phosphoryl)-5-methyl-1-pyrroline N-oxide (CYPMPO, 8 mM) in H_2O/CH_3OH (50/50/, v/v) solution containing **IrL** (500 μM, DMSO) and NADH (10 mM, H_2O) under 390 nm irradiation (10 min). The instrument is set as follows: field modulation is 2.0 G, microwave power is 5 mW, x-band frequency is about 9.63 GHz, 13 dB microwave attenuation, time constant is 1.28 ms, scanning time is 1 second, conversion time is 0.5 ms.

Cell lines and culture conditions

Cells were originally sourced from American Type Culture Collection (ATCC). 4T1 and EMT6 cells were grown in RPMI 1640 medium supplemented with 10% heat-inactivated fetal calf serum (FBS) and 1% penicillin/streptomycin. Cells were incubated in a humidified incubator at a constant temperature of 37°C, provided with 5% CO_2.

Cellular uptake

4T1 cells were seeded in glass-bottomed 35 mm confocal culture dishes and incubated overnight. To determine the optimal incubation concentration, cells were treated with varying concentration (10, 20, 30, or 40 μM) of **IrL** for 4 h. Subsequently, the cells were washed three times with PBS and immediately imaged using a Leica *Stellaris 5* confocal microscope. For the optimal incubation time, cells were treated with 30 μM of **IrL** for different time (0.5 h, 1 h, 2 h, or 4 h). Then, the cells were washed three times with PBS and imaged by Leica *Stellaris 5* confocal microscope.

Intracellular localization

4T1 cells were plated in confocal culture dishes and left to incubate overnight or cell attachment. Cells were incubated with **IrL** (30 μM) for 4 h, and then incubated with Lyso-Tracker Green (50 nM, 60 min) or Mito-Tracker Red (50 nM, 20 min), respectively. Afterwards, the cells were washed three times with PBS and observed by laser confocal microscopy. $\lambda_{ex}/\lambda_{em}$: **IrL** is 405 / 580 ± 20 nm, Lyso-tracker is 488 / 520 ± 20 nm, Mito-tracker is 561 / 640 ± 20 nm. EMT6 cells follow the same steps and procedures. For co-localization of **IrL** and LTG and MTR, cells were incubated with **IrL** (30 μM) for 4 h and further stained with 50 nM MTR and LTG.

ICP-MS assays

EMT6 cells were cultured in 100 mm Petri dishes (Costar) overnight to facilitate cell attachment. Following this, the cells were exposed to **IrL** (30 μM) for 4 h at 37°C in a 5% CO_2 atmosphere. Subsequently, the cells were washed with PBS, detached using trypsin, and counted before being divided into two equal portions. One portion was subjected to lysosome extraction as per the manufacturer's instructions provided with a lysosome extraction kit from Solaibao (Beijing, China). while the other portion underwent mitochondrial extraction using a mitochondrial extraction kit from the same manufacturer. Each cellular fraction was then treated with 60% nitric acid. Each cellular fraction underwent treatment with 60% nitric acid (HNO_3) and was allowed to digest at ambient temperature for a duration of 24 h. Following this, the samples were diluted using ultrapure water to achieve a final HNO_3 concentration of 2%. The quantification of iridium was carried out using inductively coupled plasma mass spectrometry (ICP-MS). Duplicate measurements were taken for each cellular component, and these measurements were repeated in triplicate across two independent experiments to ensure precision. The variability in measurements was evaluated by determining the standard deviation for each set of data.

pH-dependent emission in 4T1 cells

4T1 cells were cultured in confocal culture dishes overnight to allow for cell attachment. Cells were incubated in **IrL** (30 μM) for 4 h. After a single wash with PBS, the cells were exposed to different PBS buffer solutions at pH 5.0, 6.5, and 7.4.

Subsequently, the cells were co-incubated with Nigerian bacteriocin (20 μM) for 10 min and immediately visualized by confocal microscopy.

Calcein AM /propidium iodide double staining

4T1 cells were seeded into confocal culture dishes and cultured overnight. After incubation with **IrL** (30 μM) for 4 h, the cells were then co-incubated with both Ca-AM (10 μM) andPI (5 μM). The cells were subjected to light irradiation (390 nm, 45 mW cm^{-2}, 20 min) or no light treatment, followed by incubation at 37°C for 15 min and direct observation by confocal microscopy (Leica *Stellaris 5*). For the NaN_3 group, cells were incubated with NaN_3 (10 mM) for 1 h prior to the addition of Ca-AM (10 μM) and PI (5 μM), and the subsequent treatments were the as for other groups. For Ca-AM, the excitation wavelength was set at 488 nm and the emission were collected from 500-540 nm. For PI, the excitation wavelength was set at 561 nm and the emission were collected from 600-640 nm.

Annexin V-FITC/PI assay

4T1 cells were seeded in confocal culture dishes and allowed to adhere overnight. 4T1 cells were treated with **IrL** (30 μM) for 4 h in the dark. For light treatment, the 4T1 cells were then irradiated with an LED light source (390 nm, 45 mW·cm^{-2}) for 20 min. For the NaN_3 group, the cells were incubated with NaN_3 (10 mM) for 1 h before light treatment. The cells were washed three times with PBS. Addition of 500 μL of annexin-binding buffer, followed by incubation with 5 μL Annexin V-FITC and 10 μL PI stock solution for 20 minutes at room temperature, protected from light. Images were obtained on a Leica *Stellaris* 5 confocal microscope.

Cellular ROS detection

The production of intracellular ROS was detected by DCFH-DA. 4T1 cells were inoculated in confocal culture dishes overnight. After **IrL** (30 μM) treatment of the cells for 4 h, the cells were washed once with PBS and the cells were further incubated with 10 μM DCFH-DA for 20 min at 37°C in the dark. Then the cells were irradiated with a 405 nm laser (0.11%) and images were captured using a Leica *Stellaris* 5 confocal

microscope immediately after every 3 min of irradiation. The excitation/emission wavelengths used for imaging were 488/520 nm.

Acridine Orange (AO) staining

4T1 cells were plated into confocal dishes overnight for cell adherence. Following incubation in various concentration (15 μM, 30 μM, 60 μM) of **IrL** for a duration of 4 h, the cells were subjected to irradiation using light of 390 nm (45 mW cm^{-2}) for 15 min, or they were kept in dark conditions. Subsequently, the cells were washed thrice with PBS and incubated in 5 μM Acridine Orange (AO) at 37°C for 15 min. Then the cells were visualized using Leica *Stellaris 5* confocal microscopy. Under the excitation of 488 nm, the fluorescence was collected at 510 ± 20 nm (green) and 625 ± 20 nm (red).

To visualize the lysosomal integrity of PDT-treated 4T1 cells more visually, the cells were treated with **IrL** (30 μM) for 4 h, washed three times with PBS, and incubated with AO (5 μM) for 15 min at 37 °C. Then, the cells were irradiated with a 405 nm laser (at 2% intensity), and the images were captured using a confocal microscope (Leica *Stellaris 5*) every 40 s of irradiation.

Co-culture of EMT6 cells and BHK-21 cells

EMT6 cells were seeded into confocal culture dishes with similar amount of BHK-21 cells, and incubated for 24 h. The cell mixtures were exposed to **IrL** (30 μM) for 4 h and then co-stained with both Ca-AM (10 μM) and PI (5 μM). Then the cells were irradiated with a 405 nm laser (5%) for 5 min, and images were captured using a Leica *Stellaris* 5 confocal. $\lambda_{ex}/\lambda_{em}$: **IrL** is 405 / 580 ± 20 nm, Ca-AM is 488 / 520 ± 20 nm, PI is 561 / 620 ± 20 nm.

Detection of cathepsin B release

4T1 cells were inoculated into confocal dishes overnight for cell adhesion. Cathepsin B activity according to Magic Red® Cathepsin-B Assay Kit (Immunochemistry Tech). Cells were incubated in **IrL** (30 μM) for 4 h, then irradiated at 390 nm (45 mW cm^{-2}) for 20 min or darkened, washed three times with PBS, incubated with cathepsin B substrate for 50 min, washed twice with PBS, as observed by confocal microscopy

(Leica *Stellaris 5*). $\lambda_{ex}/\lambda_{em}$: **IrL** (red) is 405/580 nm, Cathepsin B (green) is 561/630 nm.

JC-1 staining

4T1 cells were inoculated into confocal dishes overnight for cell attachment. The mitochondrial membrane potential was determined by JC-1 dye. After incubation in **IrL** (30 μM) for 4 h, the cells were irradiated with 390 nm light (45 mW cm^{-2}) for 20 minutes or dark treatment, rinsed three times with PBS, and then incubated in JC-1 (10 μg/ml) for 20 minutes, rinsed three times with PBS, and visualized under a confocal microscope (Leica *Stellaris 5*). In the positive control group, 4T1 cells were exposed to FCCP (10 μM) for 1 h and then incubated with JC-1 (10 μg/ml) for 20 min. $\lambda_{ex}/\lambda_{em}$: J-aggregates (red fluorescence) is 561/585 nm, J-Monomer (green fluorescence) is 488/529 nm.

Caspase-3/7 activity assay

Caspase-3/7 activity was measured using the Caspase-Glo® Assay kit (Promega, USA) according to the manufacturer's instructions. 4T1 cells were cultured in 96-well plates and treated with **IrL** (10 μM) for 4 h at 37℃ in the dark. For light treatment, the 4T1 cells were then irradiated with an LED light source (390 nm, 45 mW·cm^{-2}) for 20 min followed by recovery for 0.5 h. 100 μL Caspase-Glo® 3/7 reagent was added to each well containing 100 μL culture media. The mixture was incubated at room temperature for 1 h and then the luminescence was measured using a microplate reader (Varioskan LUX, Thermo Fisher Scientific, USA).

Cytotoxicity assay

The cytotoxicity of **IrL** were assessed in 4T1 cells and EMT6 cells using MTS assays. For dark cell viability of **IrL**, cells were seeded in 96-well plates at a density of 1×10^4 cells/well and allowed to grow for 24 h. **IrL** were subsequently added to the wells at different concentrations (0, 0.1, 0.25. 0.5, 1, 2.5, 5, 10, 20, 30, 40, 50, 75, 125, 200 μM), respectively. After 48 h incubation, 10 μL MTS stock solution (CellTiter 96 AQueous One Solution Cell Proliferation Assay) was added to each well for another 3 h under the same conditions. Then the absorbance at 500 nm was measured by a SpectraMax 190 Microplate Multimode Reader.

For phototoxicity, cells were incubated with different concentrations of **IrL** for 4 h. Cells were then irradiated with 390 nm light (45 mW cm^{-2}) for 30 min and incubated for another 41 h. After adding 10 μL of MTS solution, the cells were incubated for another 3 h. The absorbance at 500 nm was measured using SpectraMax 190 microplate reader.

Hypoxic cytotoxicity assay

For dark toxicity and phototoxicity tests under hypoxic conditions of **IrL**, cells were inoculated at 1×10^4 cells per well into 96-well plates for 24 h at a constant temperature of 37°C providing 5% CO_2, 21% O_2 and 95% air, **IrL** were subsequently added to the wells at different concentrations (0, 0.125, 0.25. 0.5, 1, 2.5, 5, 20, 30, 75 μM), respectively. For phototoxicity under hypoxic conditions of **IrL**, after 4 h, the cells were illuminated (390 nm, 45 mW cm^{-2}) for 30 minutes, immediately placed in an MGC microaerophilic air-producing bag (AneroPack, provides about 5 % O_2 and about 5 % CO_2), placed in a cell incubator, and cultured for another 40 h. After adding 10 μL of MTS solution, the cells were incubated for another 3 h at a constant temperature of 37°C providing 5% CO_2, 21% O_2 and 95% air. The absorbance at 500 nm was measured using SpectraMax 190 microplate reader.

For dark toxicity under hypoxic conditions of **IrL**, 4 h after the addition of **IrL** (0, 0.125, 0.25. 0.5, 1, 2.5, 5, 20, 30, 75 μM), the cells were immediately placed in an MGC microaerophilic air-producing bag (AneroPack, provides about 5 % O_2 and about 5 % CO_2) and cultured for another 40 h. After adding 10 μL of MTS solution, the cells were incubated for another 3 h at a constant temperature of 37°C providing 5% CO_2, 21% O_2 and 95% air. The absorbance at 500 nm was measured using SpectraMax 190 microplate reader.

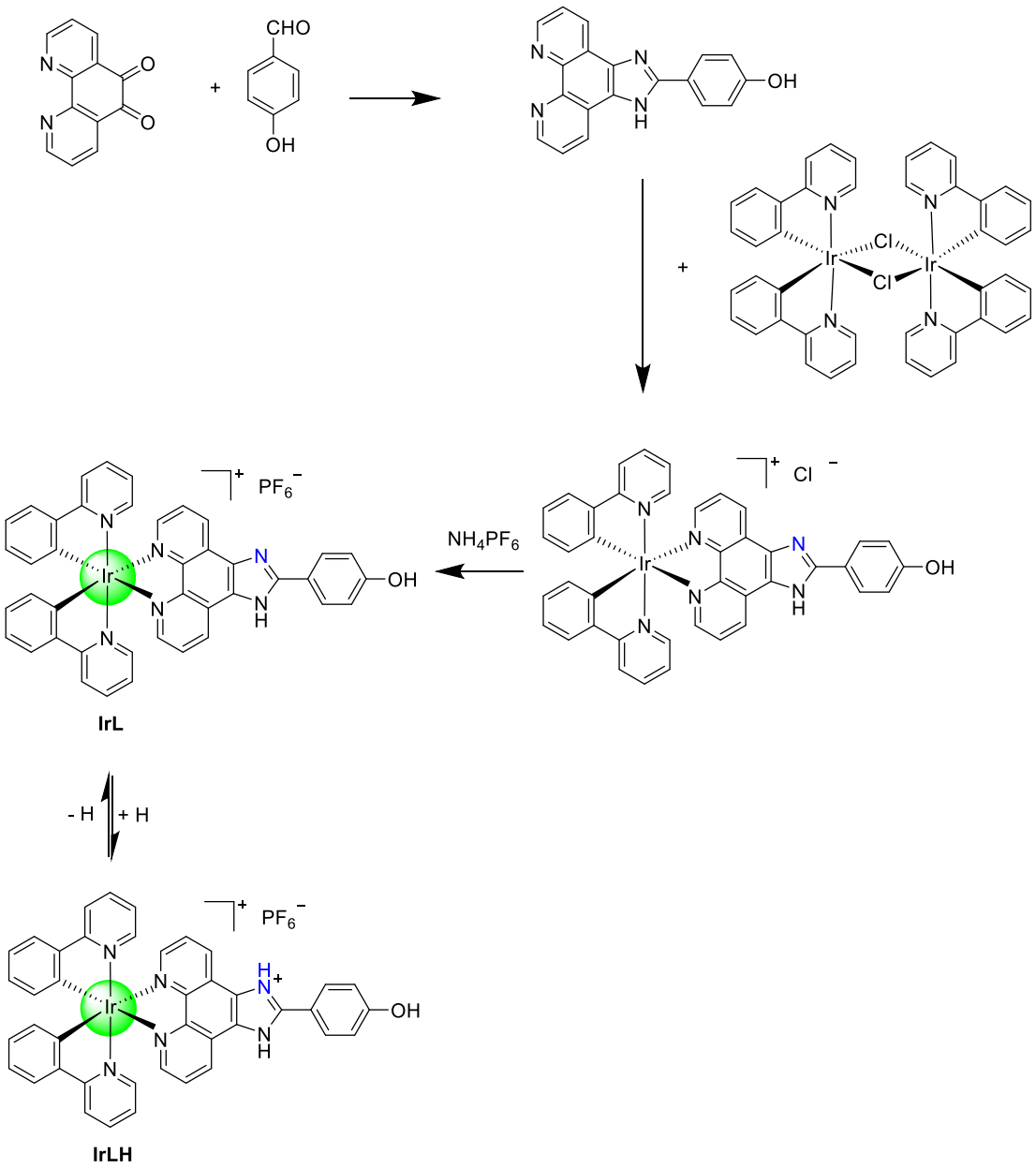

Scheme S1. Synthetic route of **IrL.**

Supporting figures

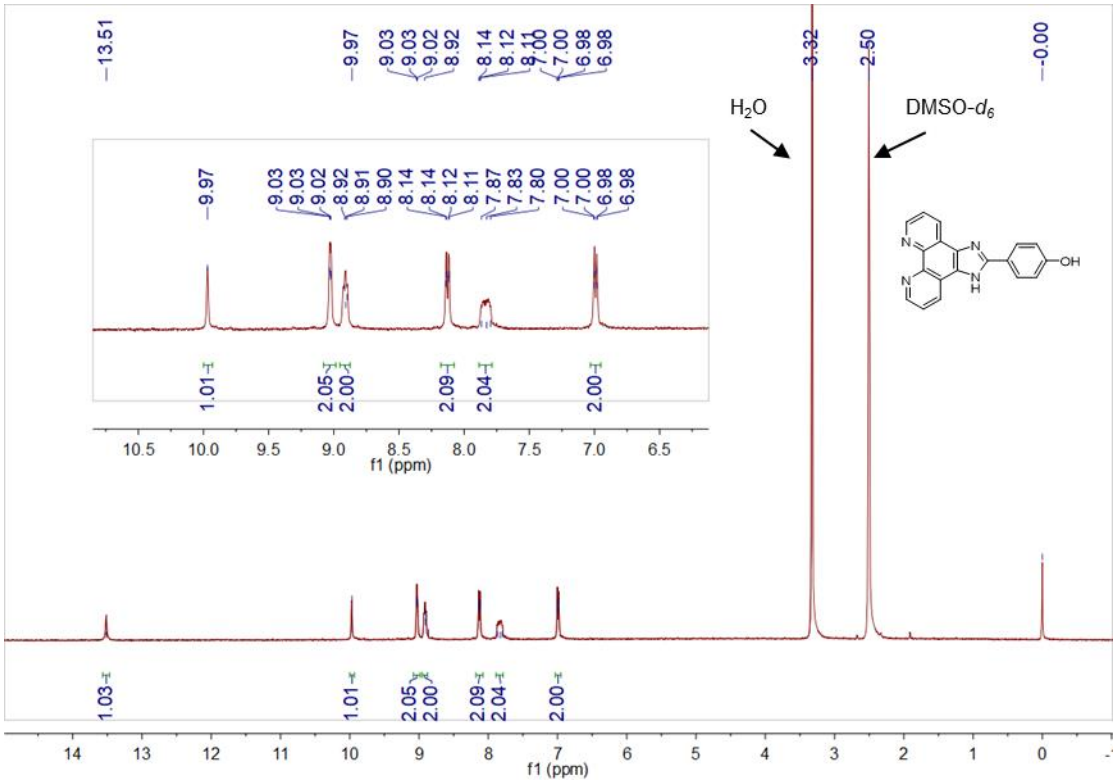

Fig. S1 ^{1}H NMR Spectrum of **L** in DMSO-d_6.

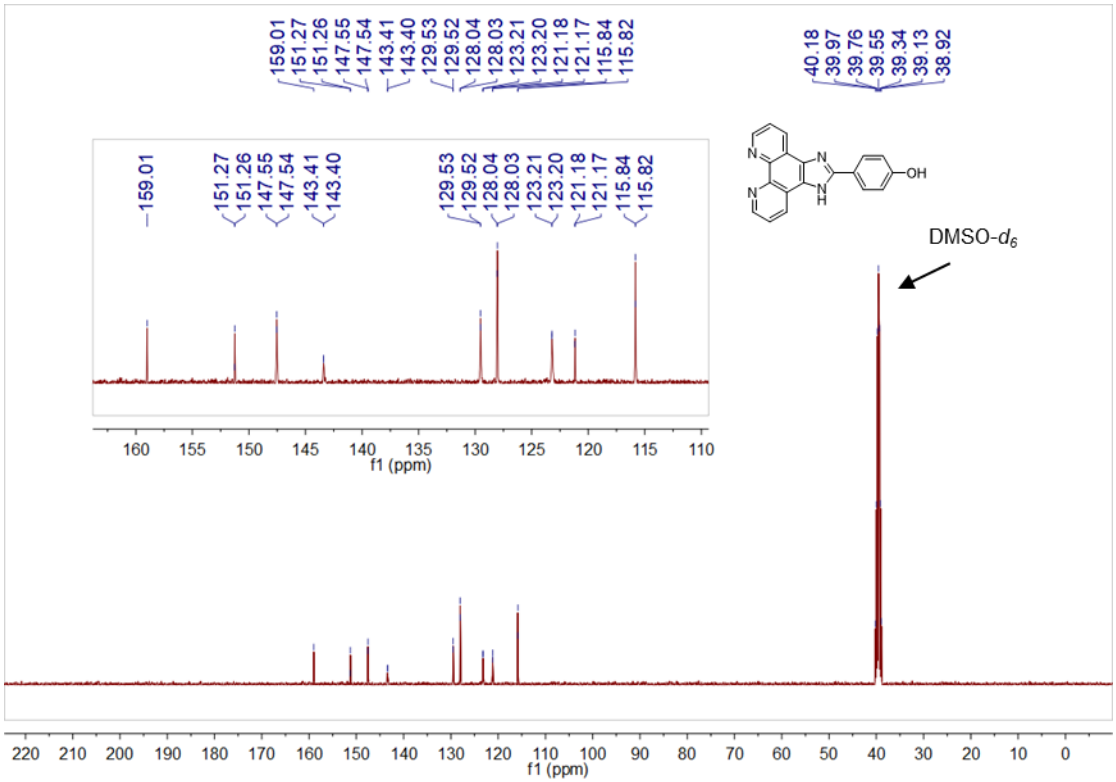

Fig. S2 ^{13}C NMR Spectrum of **L** in DMSO-d_6.

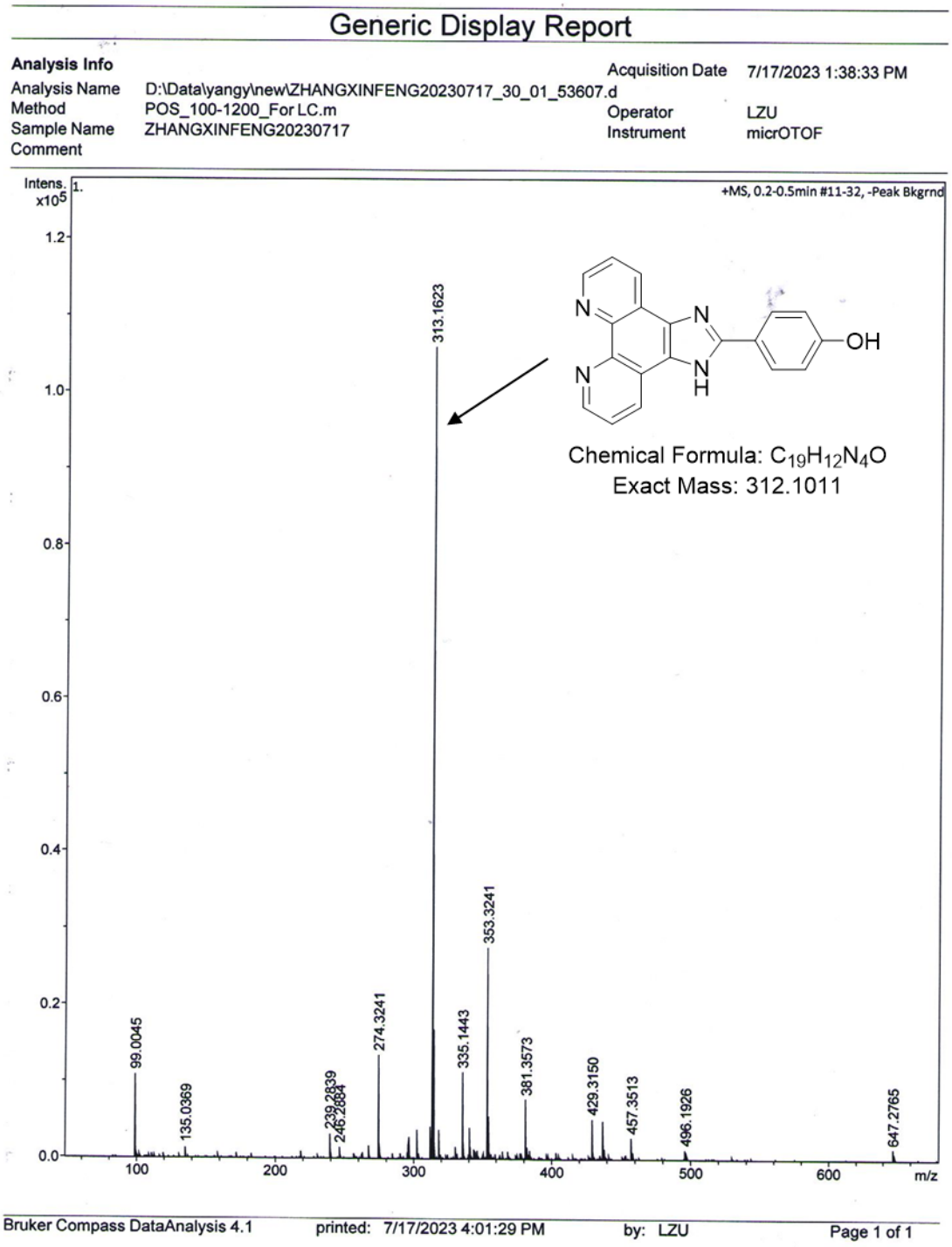

Fig. S3 ESI mass spectrum of **L**.

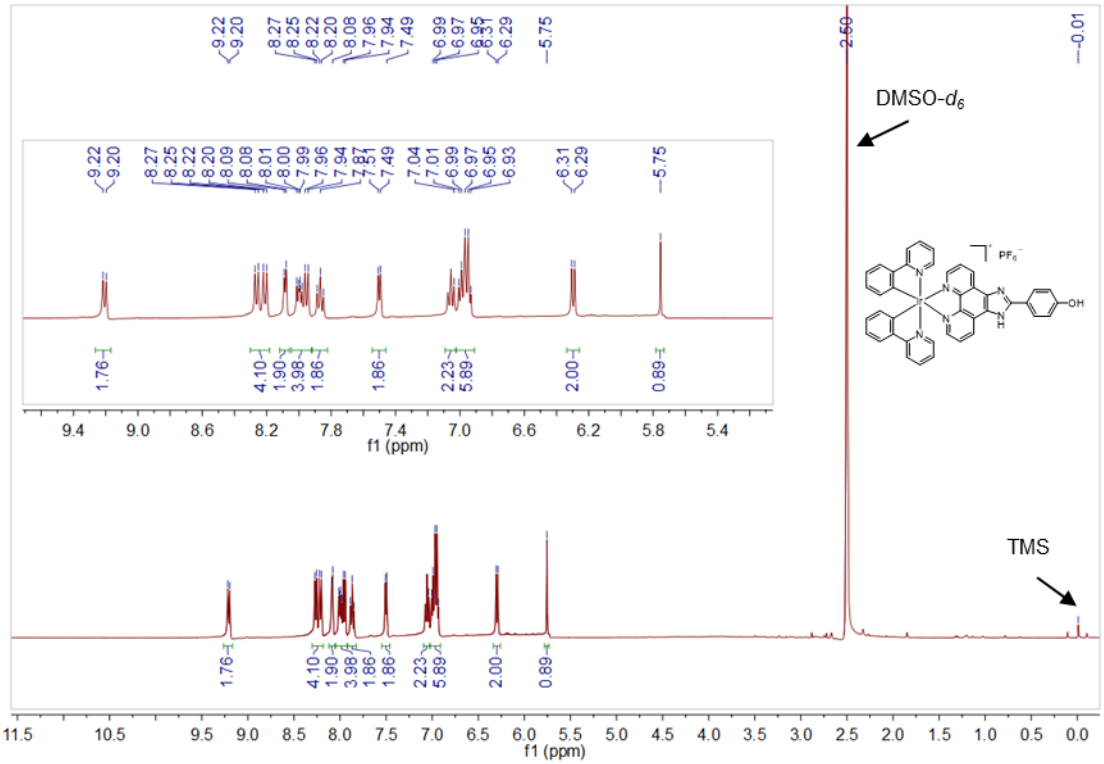

Fig. S4 ^{1}H NMR Spectrum of **IrL** in DMSO-d_6.

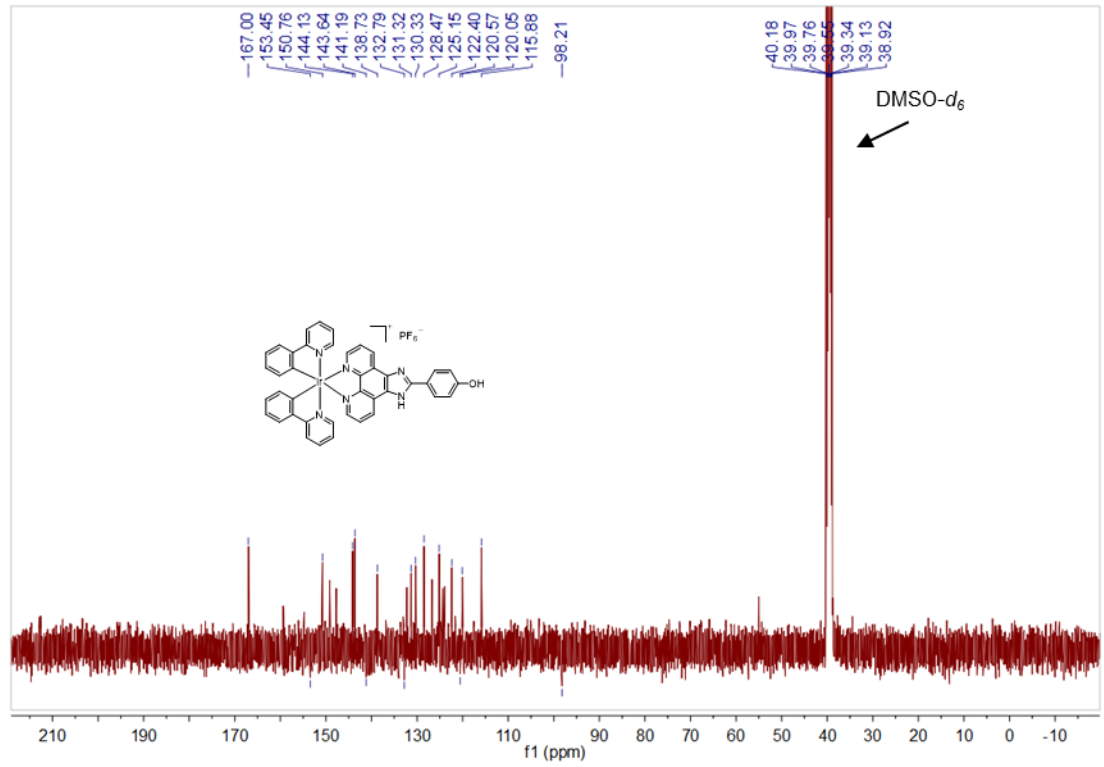

Fig. S5 ^{13}C NMR Spectrum of **IrL** in DMSO-d$_6$.

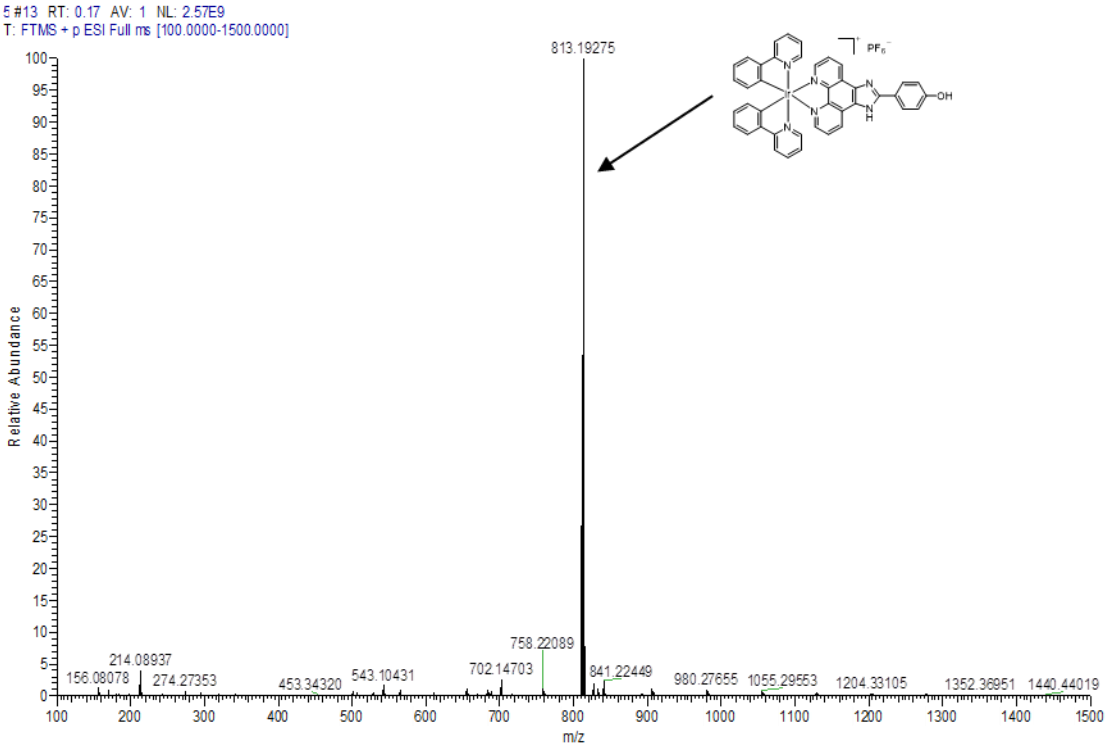

Fig. S6 ESI mass spectrum of **IrL**.

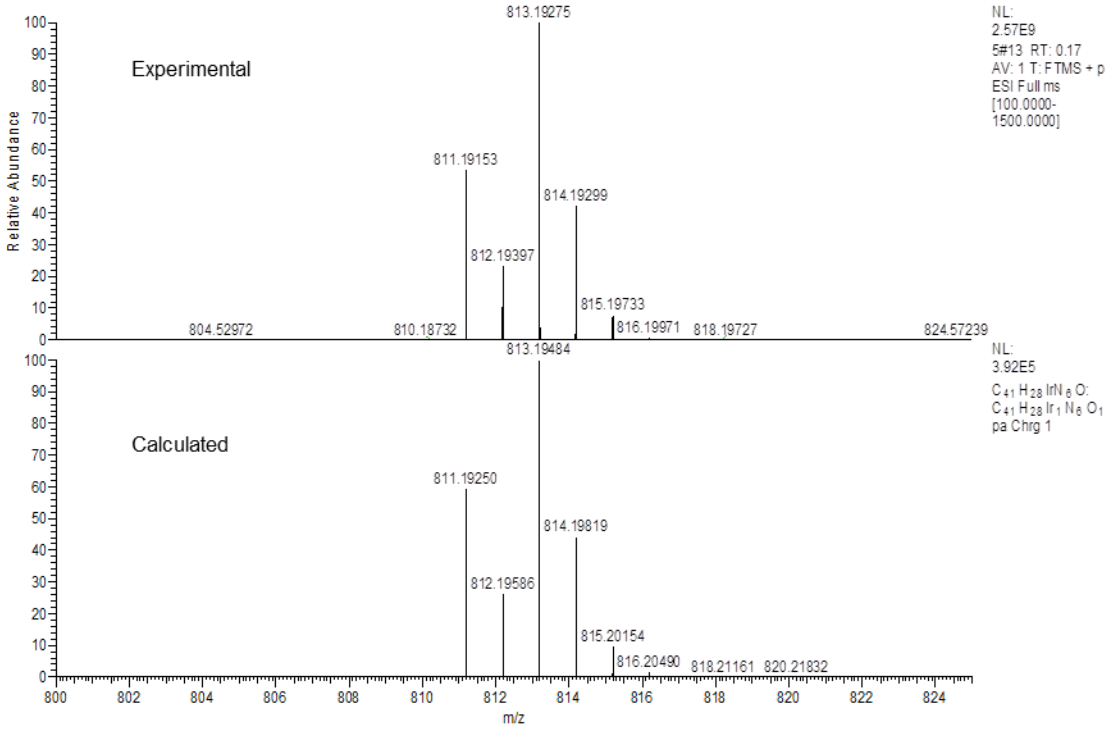

Fig. S7 ESI mass spectrum of **IrL** (The original magnification was in a range from 800 to 825).

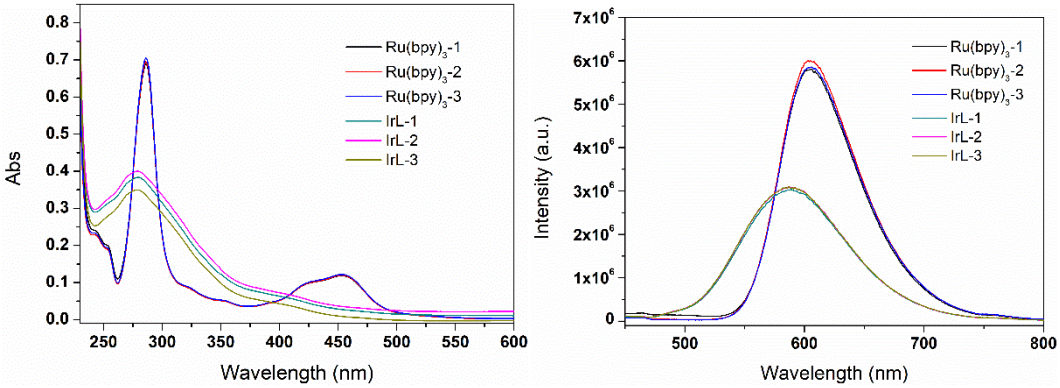

Fig. S8 UV−vis absorption (left) and emission (right) spectra of **IrL** and $[Ru(bpy)_3]Cl_2$ in DI water. Each experiment was repeated three times.

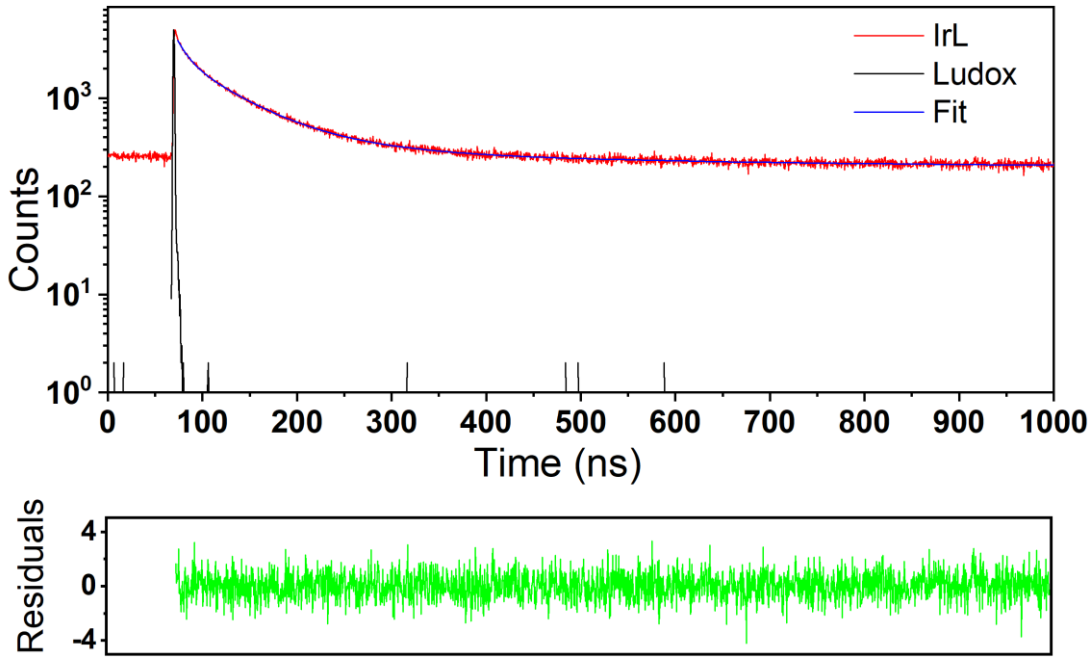

Fig. S9 Phosphorescence lifetime of **IrL**.

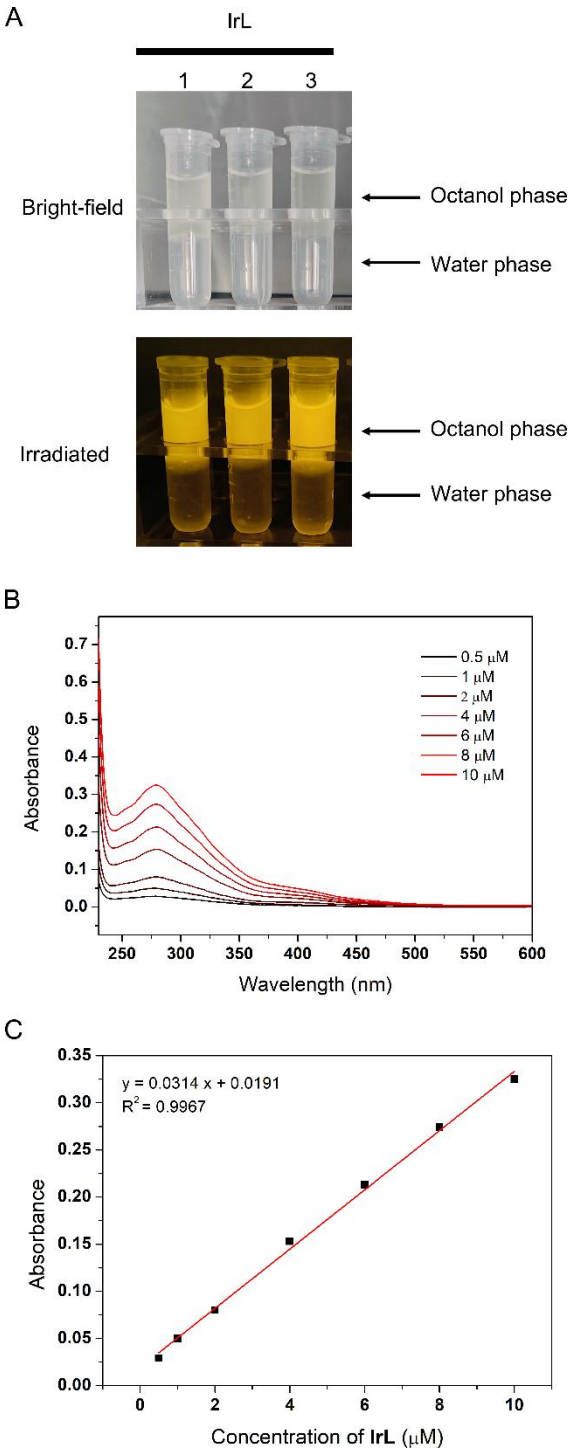

Fig. S10 Lipophilicity measurement. (A) Partition between the octanol and water phases of **IrL**. Each experiment was repeated three times. (B) Standard curves of **IrL** and fitted (C) using linear fit in Origin 8.

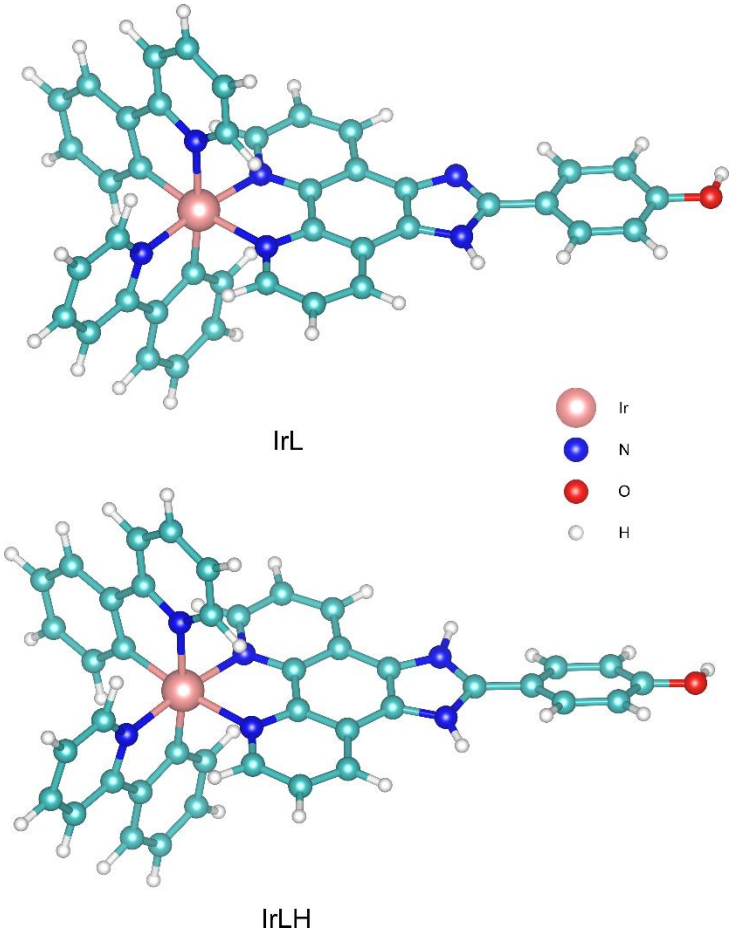

Fig. S11 Optimized structure of **IrL** and **IrLH** in the ground state with DFT method at the B3LYP level.

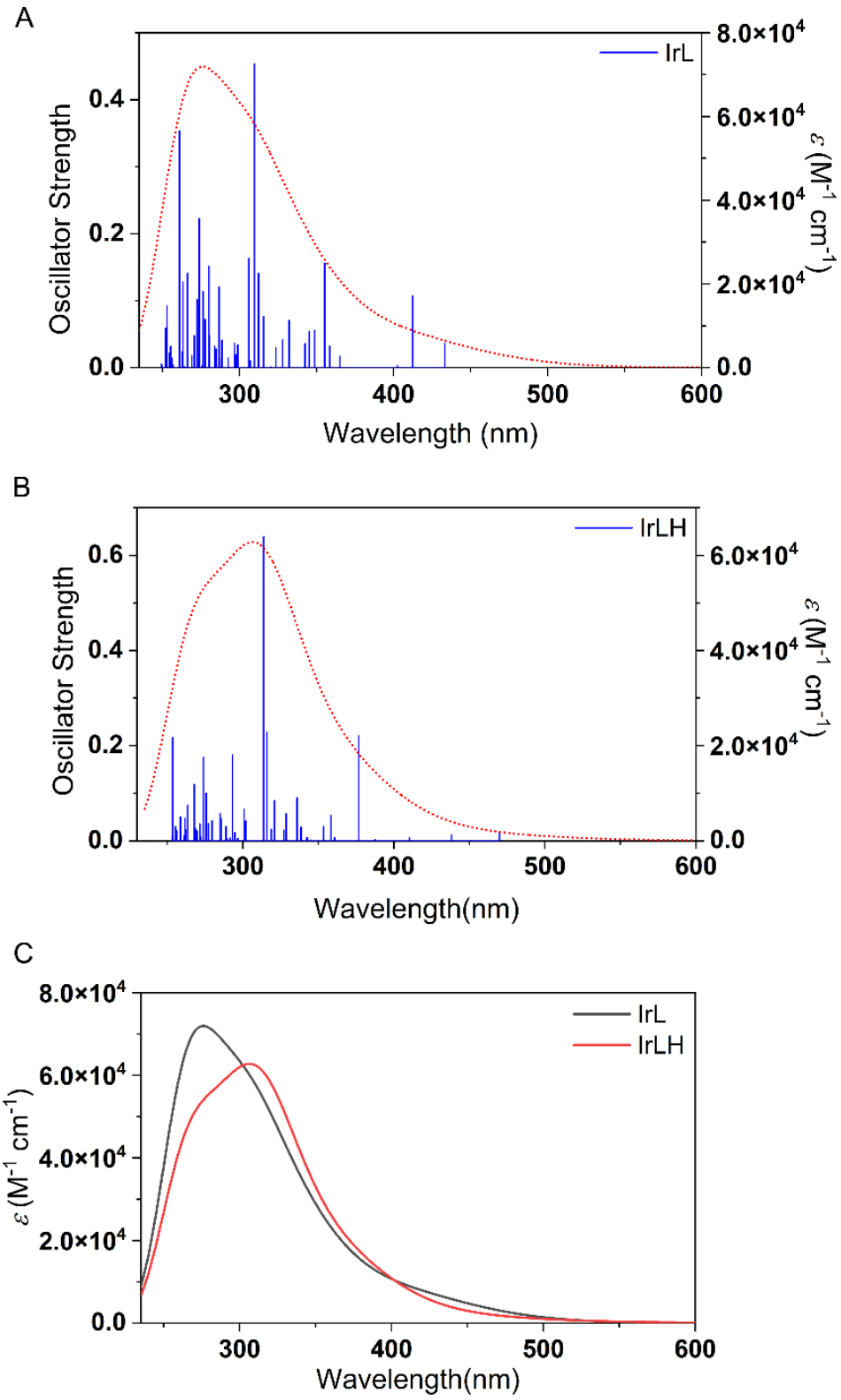

Fig. S12 Theoretical UV−vis absorption spectra of **IrL** (A) and **IrLH** (B). Blue vertical lines correspond to calculated electronic transitions whereby the height refers to the oscillator strength of the respective transition. (C) The comparison of calculated UV−vis absorption spectra between **IrL** and **IrLH**.

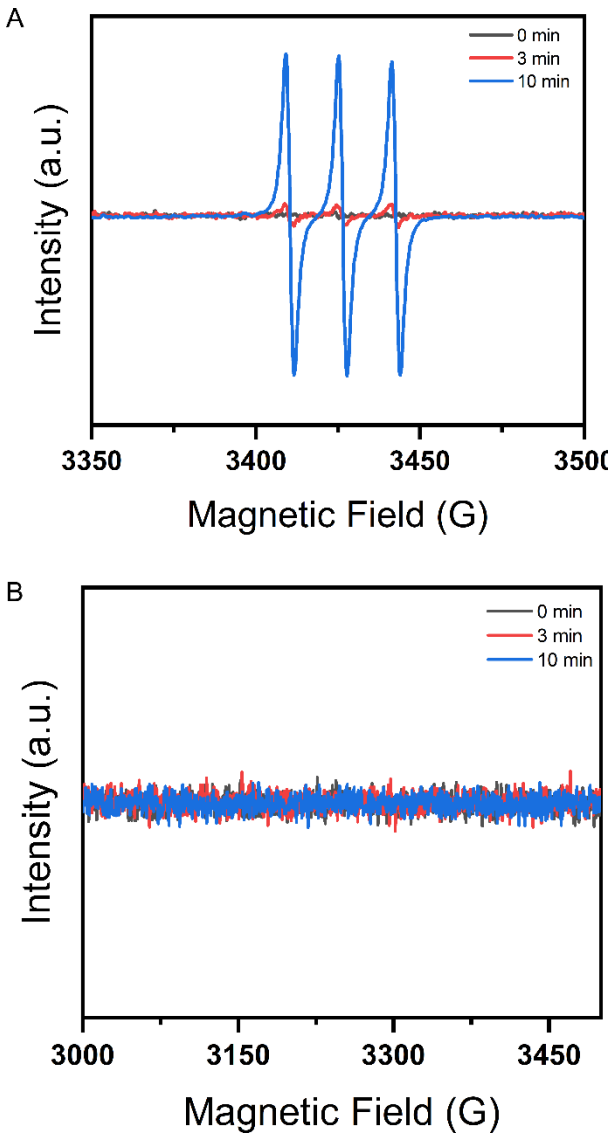

Fig. S13 (A) EPR signals of $^1O_2$ generated by **IrL** and trapped by TEMP at different times. (B) EPR signals of OH• generated by **IrL** in H_2O system and trapped by DMPO at different times. light irradiation: 390 nm, 45 mW cm^{-2}.

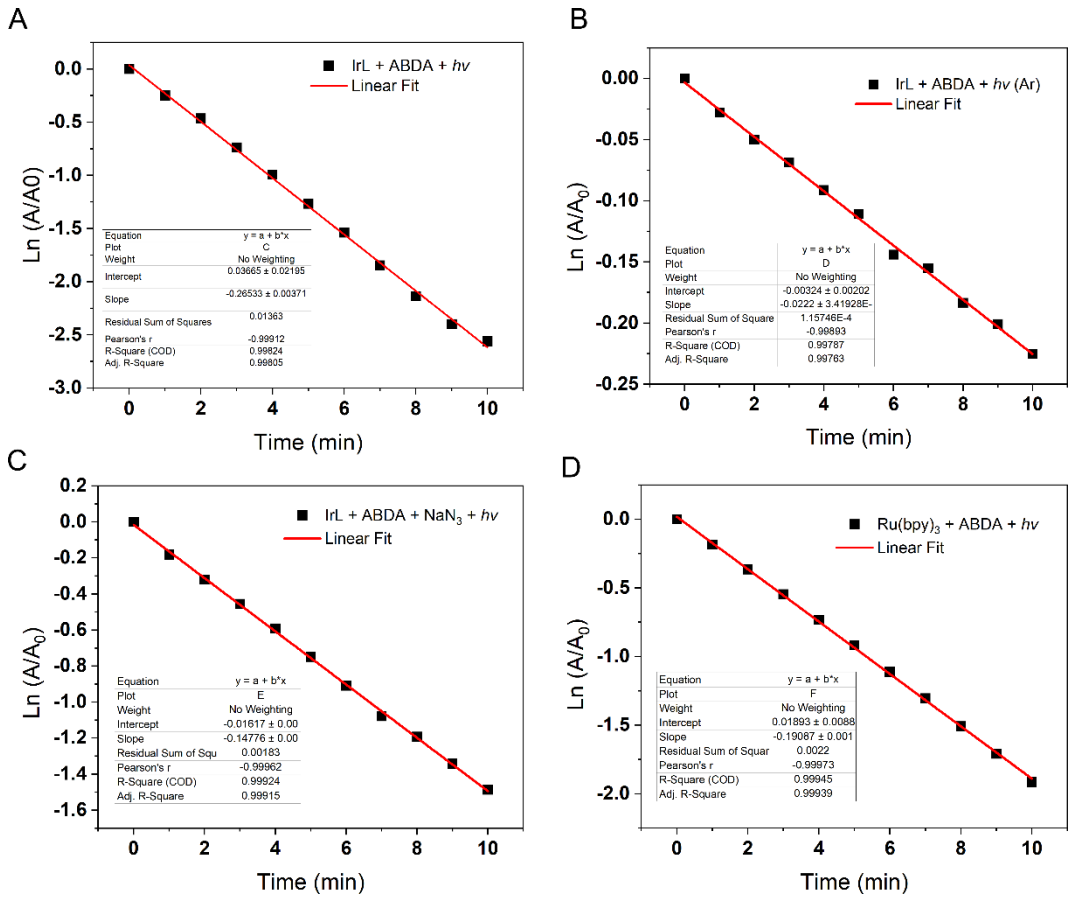

Fig. S14 Rate of decay of ABDA at 378 nm under different conditions. (A) **IrL** and ABDA in H_2O, light irradiation. (B) **IrL** and ABDA in H_2O degassed with Ar, light irradiation. (C) **IrL** and ABDA in NaN_3 aqueous solution, light irradiation. (D) $[Ru(bpy)_3]Cl_2$ and ABDA in H_2O, light irradiation. Conditions: [**IrL**] = $[Ru(bpy)_3]Cl_2$ = 10 μM, [ABDA] = 100 μM. Light irradiation = LED light (390 nm, 45 mW cm^{-2}).

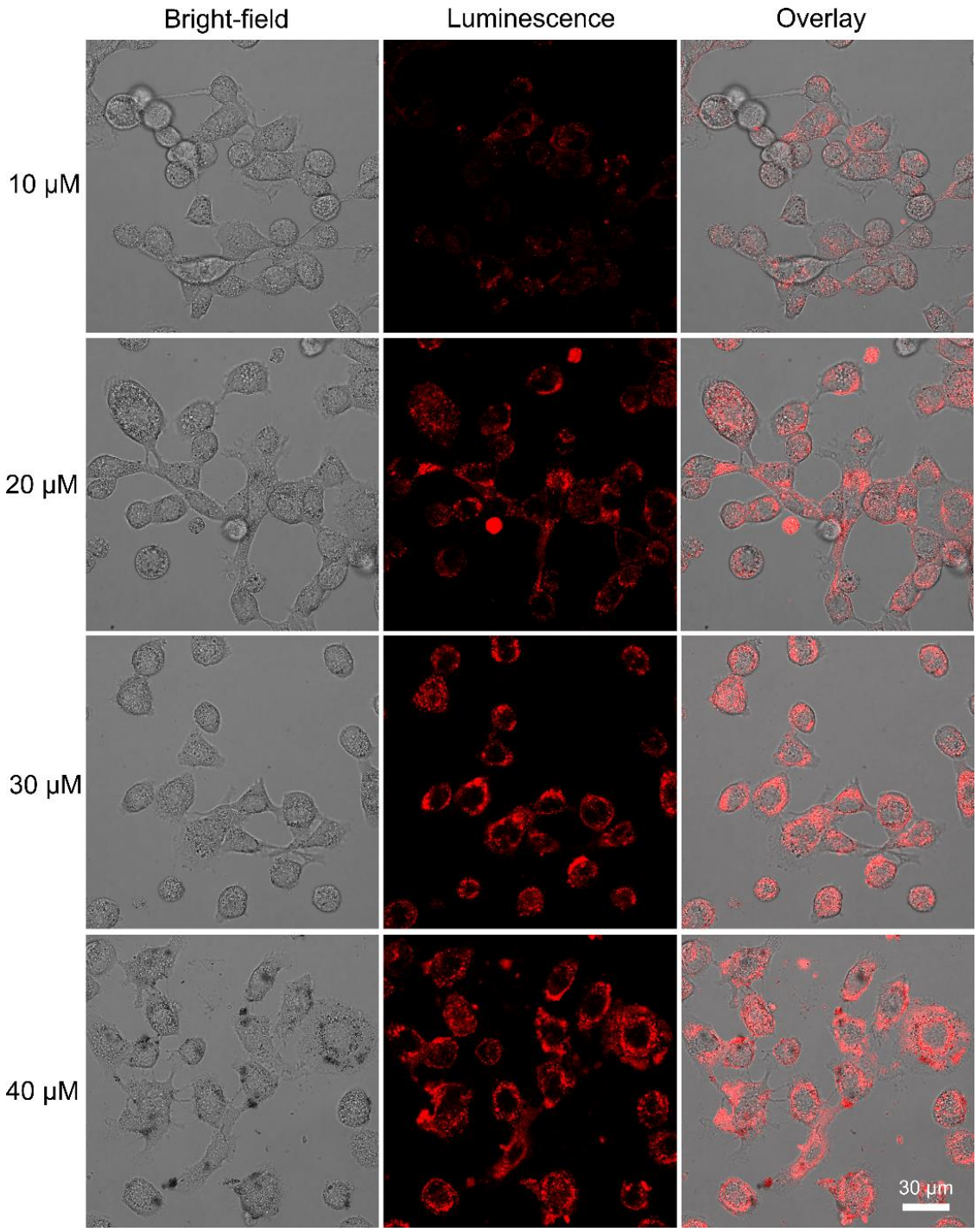

Fig. S15 Optimal incubation concentration. 4T1 cells incubated with different concentration (10, 20, 30, or 40 μM) **IrL** for 4 h at 37°C.

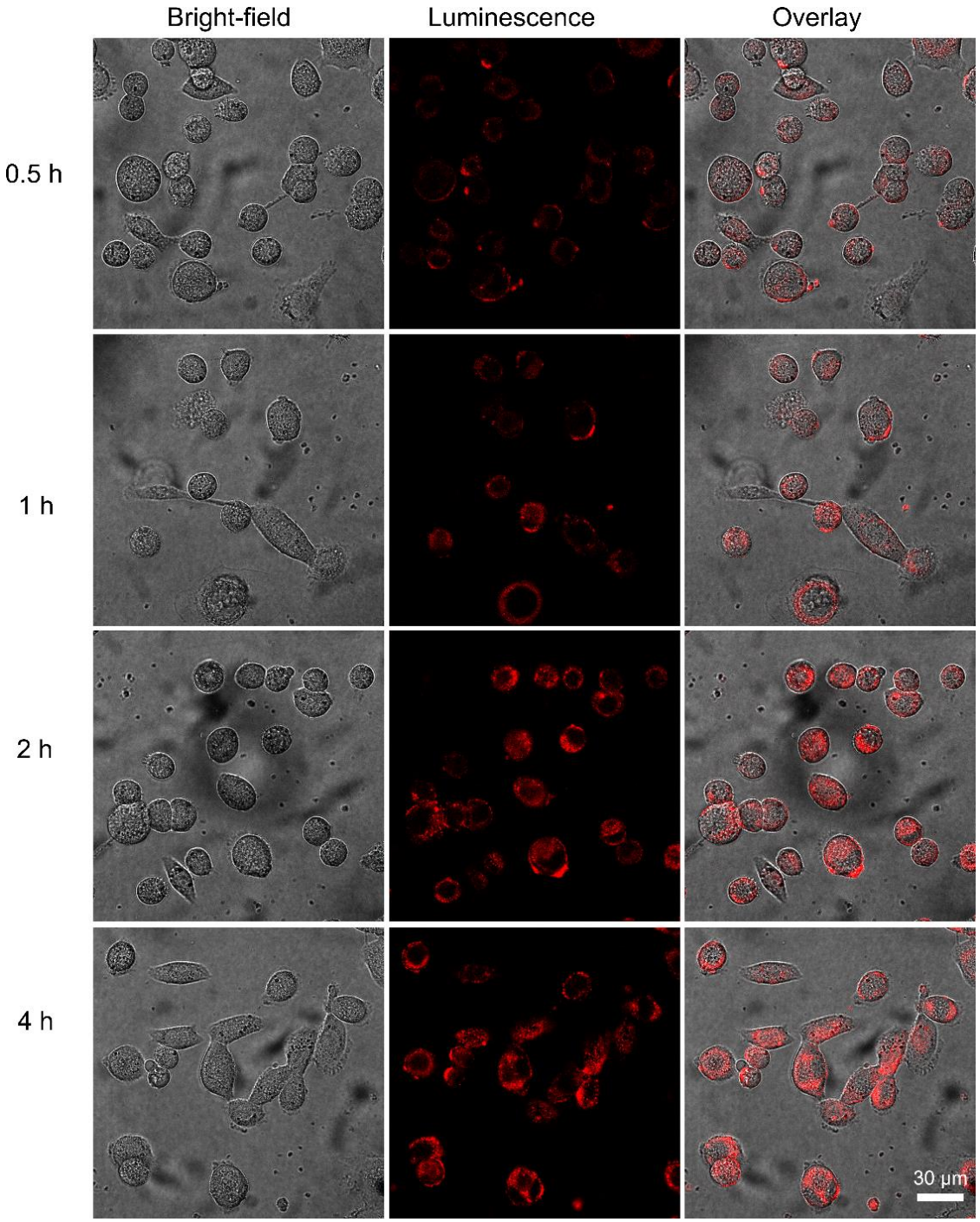

Fig. S16 Optimal incubation time. 4T1 cells incubated with **IrL** (30 μM) for different time (0.5, 1, 2, or 4 h) at 37°C.

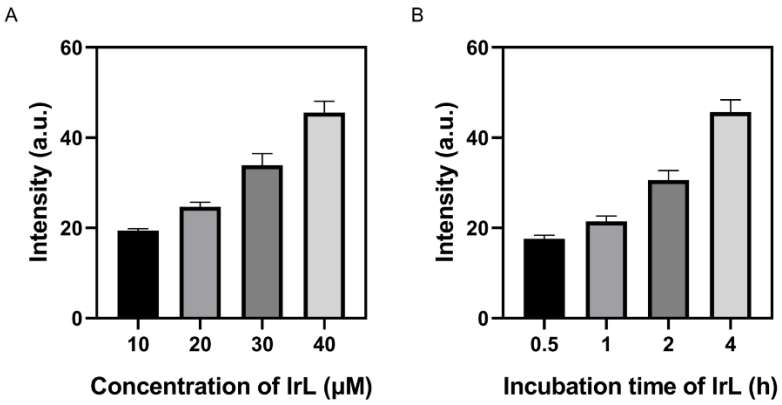

Fig. S17 The optimal incubation concentration (A) and time (B) were analyzed using Image J software.

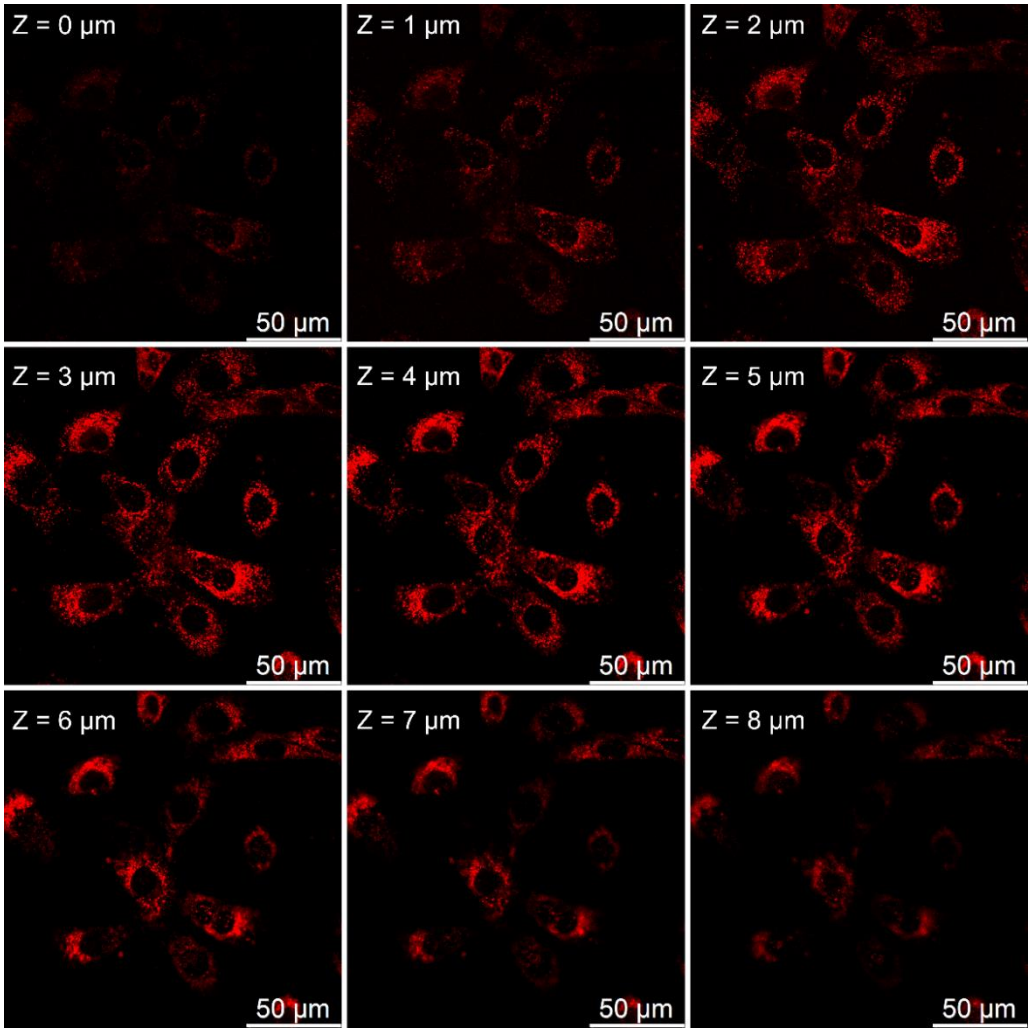

Fig. S18 Z-scan images of 4T1 cells after incubation with **IrL** (30 μM) for 4 h. Scale bar: 50 μm.

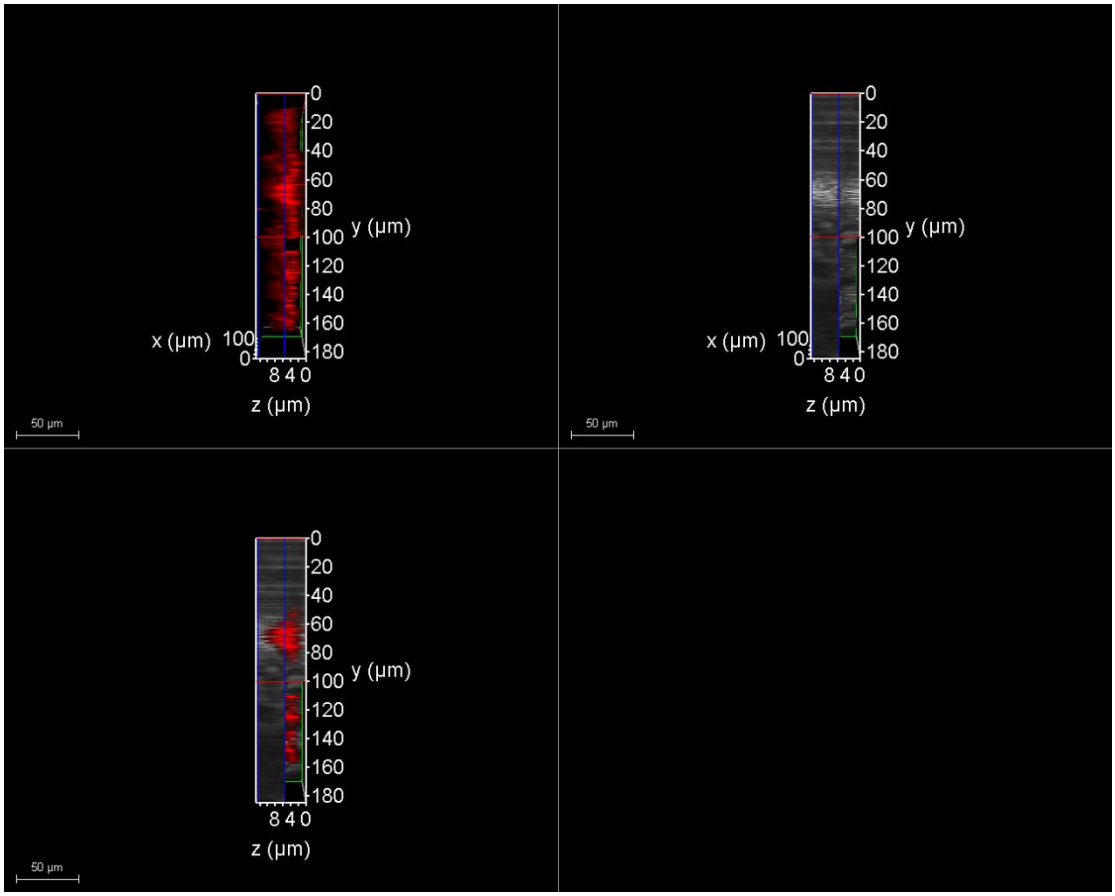

Fig. S19 Confocal microscopy YZ-axis cross-section of 3D reconstruction images of 4T1 cells were treated with the **IrL** (30 μM) for 4 h. Scale bar: 50 μm.

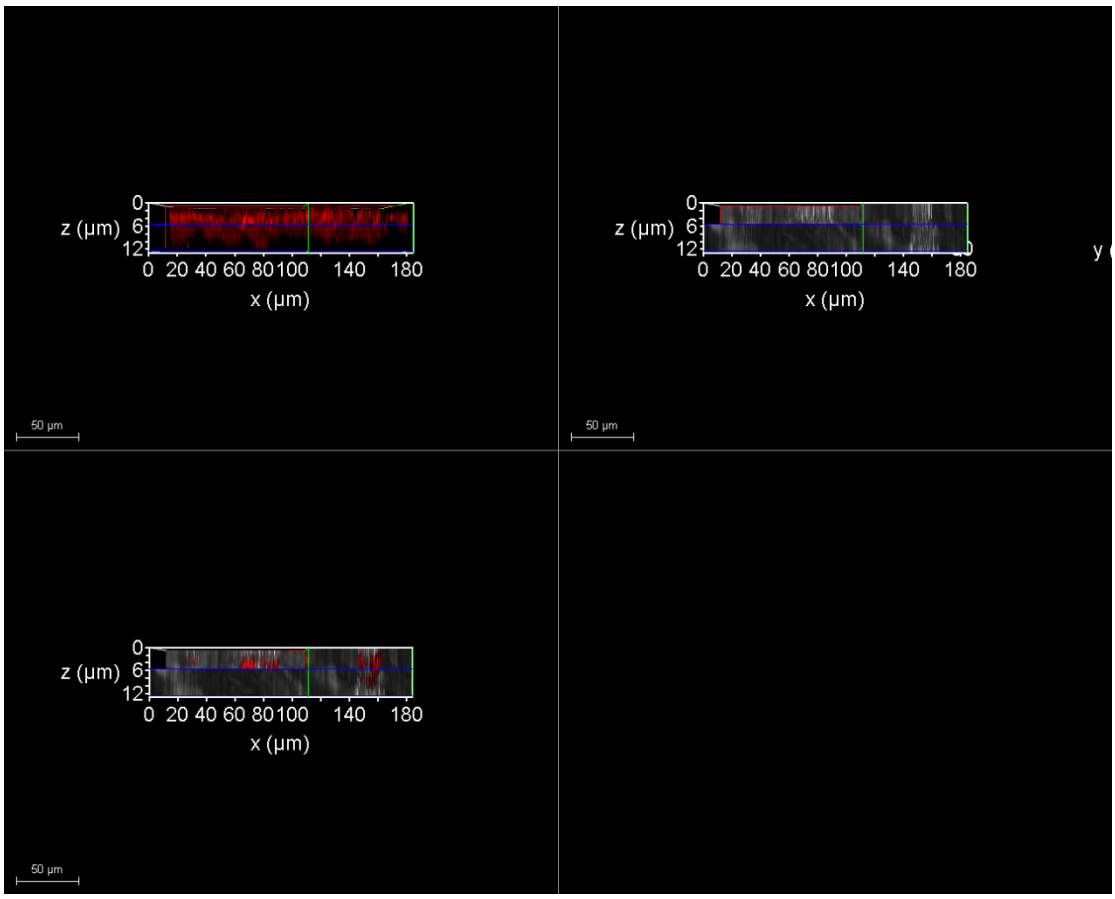

Fig. S20 Confocal microscopy XZ-axis cross-section of 3D reconstruction images of 4T1 cells were treated with the **IrL** (30 μM) for 4 h. Scale bar: 50 μm.

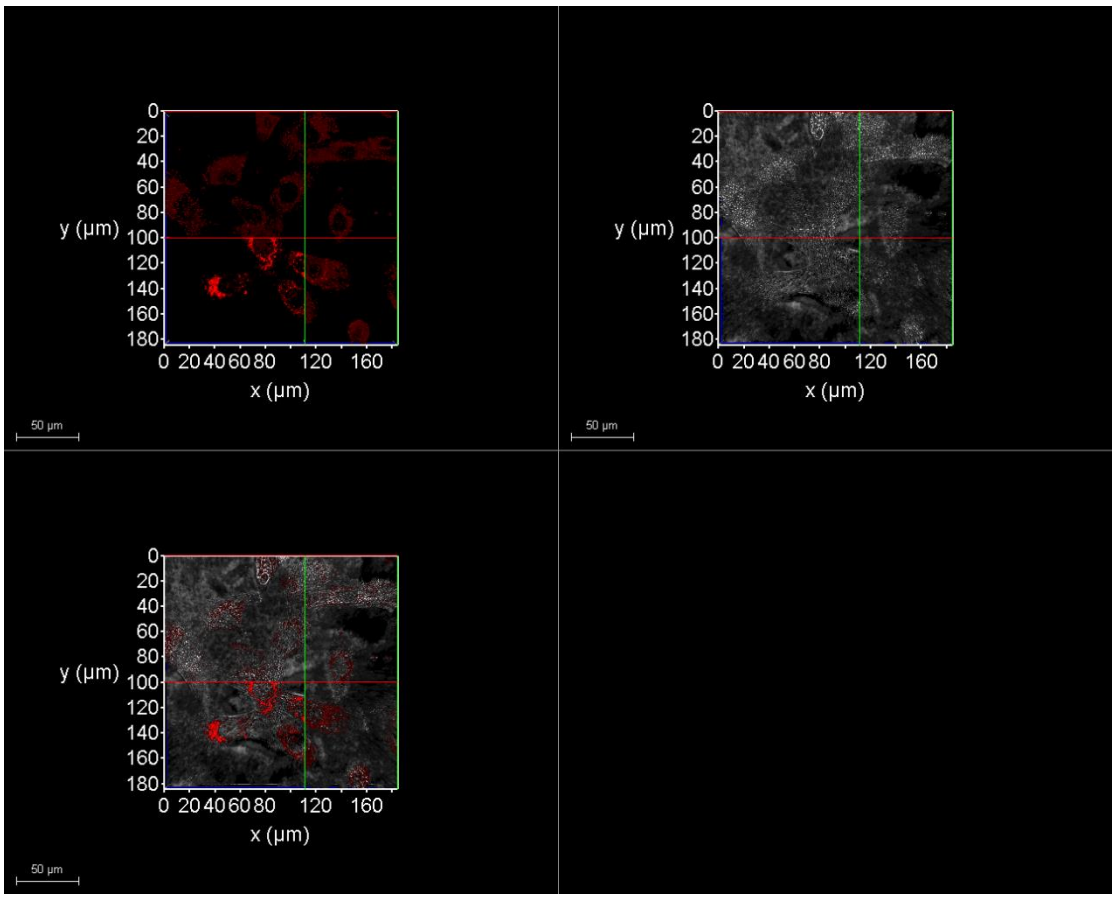

Fig. S21 Confocal microscopy XY-axis cross-section of 3D reconstruction images of 4T1 cells were treated with the **IrL** (30 μM) for 4 h. Scale bar: 50 μm.

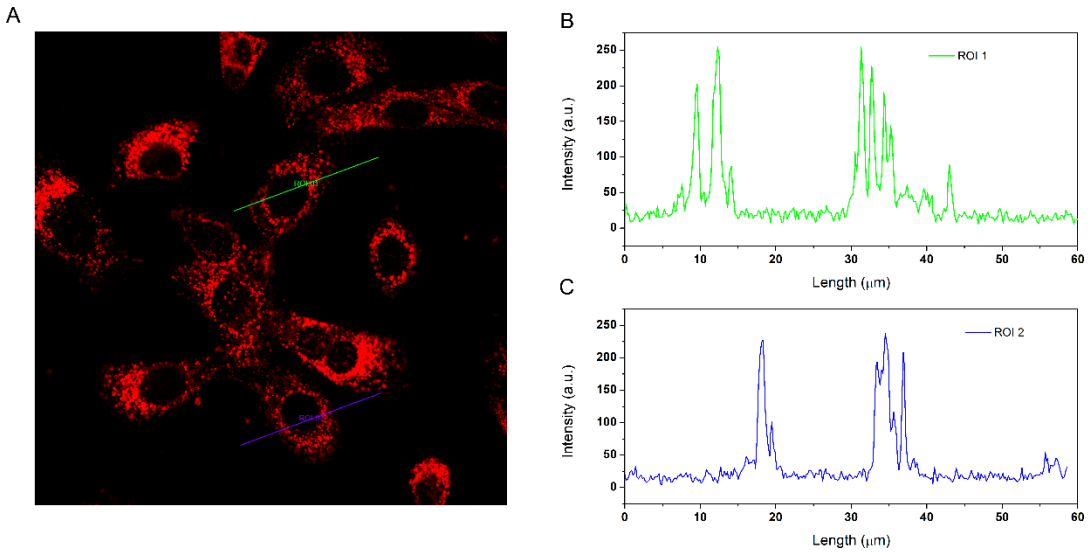

Fig. S22 Line profile intensity analysis. (A) Confocal images of 4T1 cells after incubation with **IrL** (30 μM) for 4 h. (B) ROI 1.(C)ROI 2.

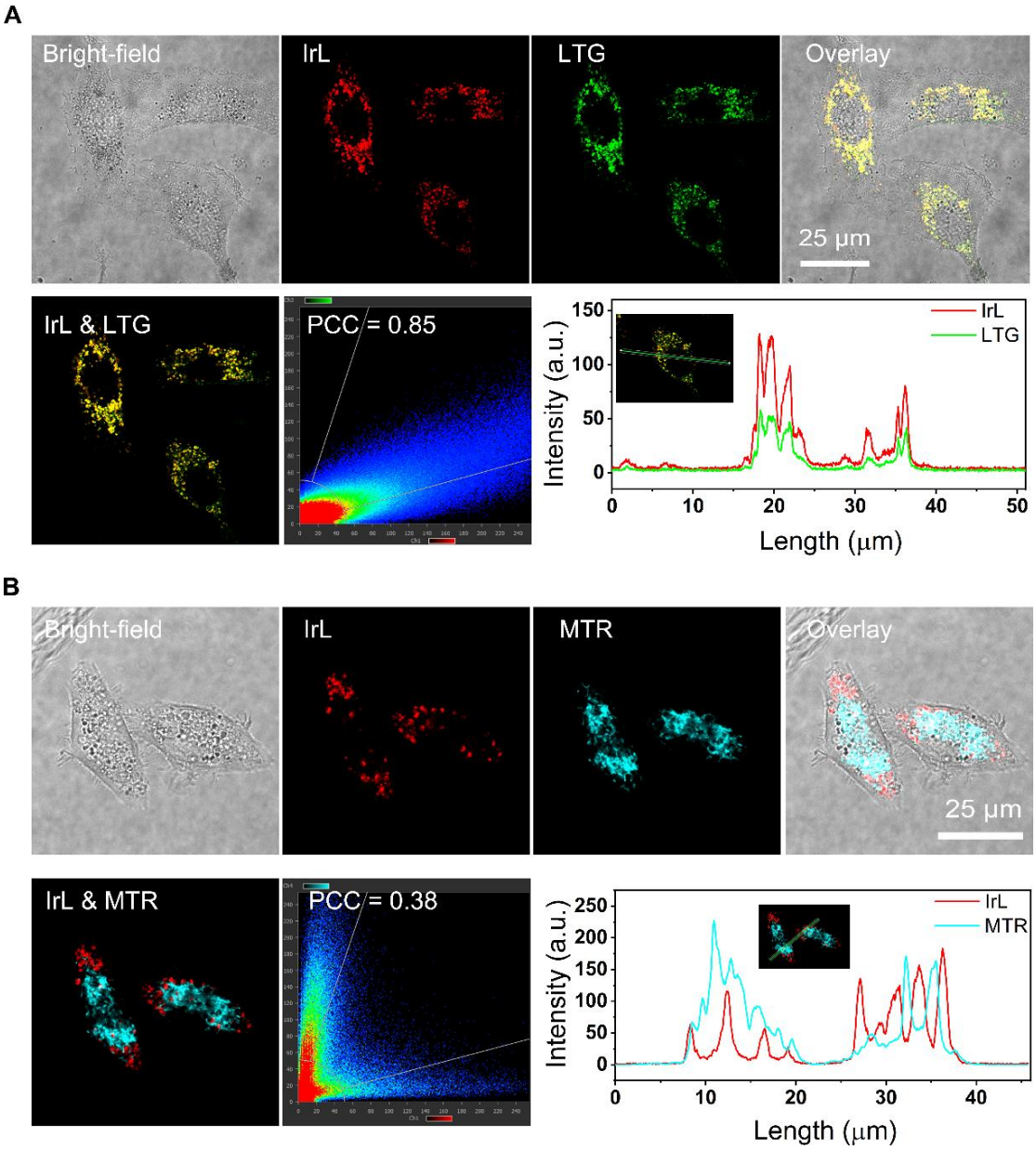

Fig. S23 Co-localization experiments of 4T1 cells. 4T1 cells were treated with **IrL** (30 μM) for 4 h, then co-stained with LTG (A, 50 nM, 20 min) or MTR (B, 50 nM, 60 min), respectively.

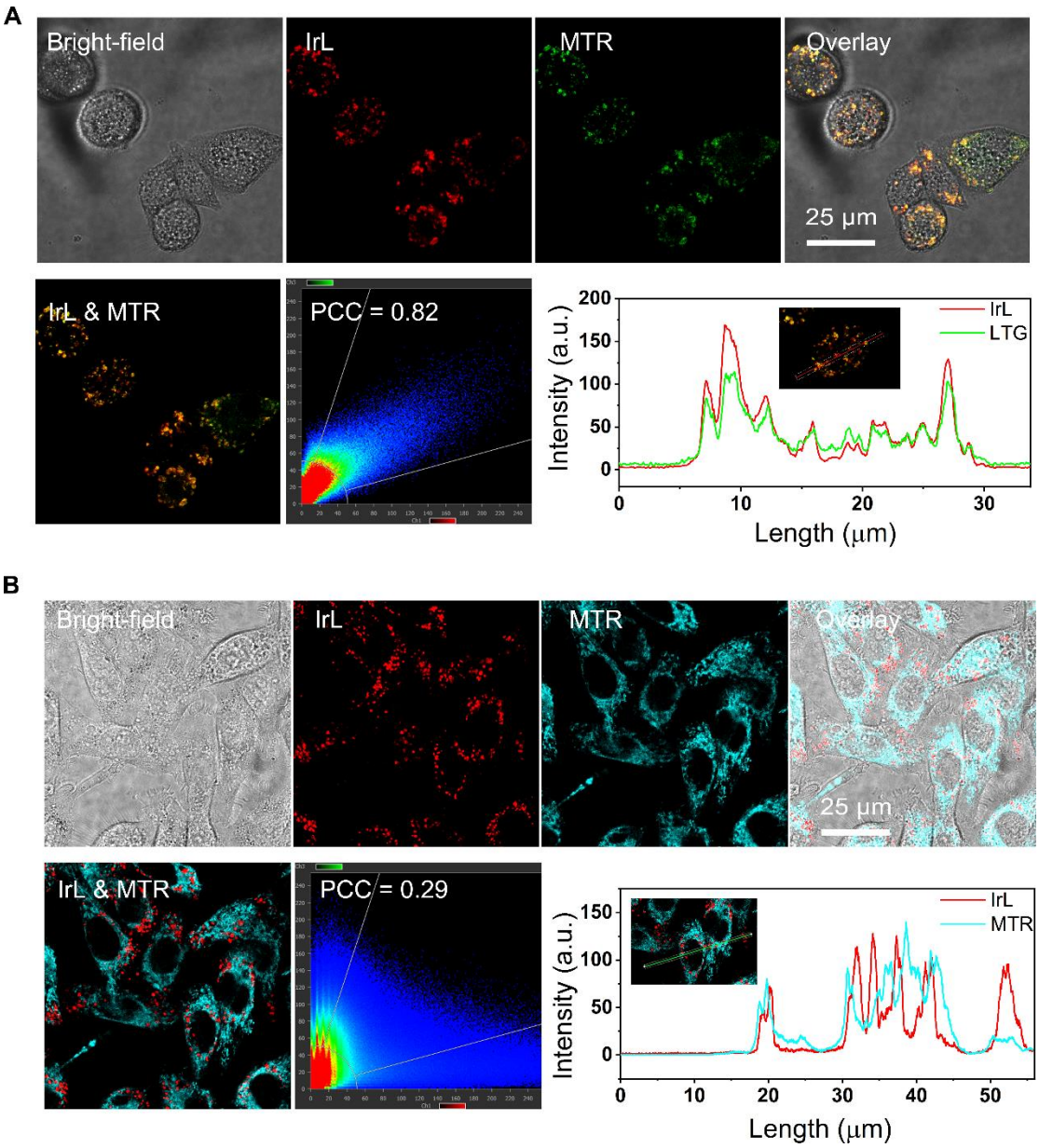

Fig. S24 Co-localization experiments of EMT6 cells. EMT6 cells were treated with **IrL** (30 μM) for 4 h, then co-stained with LTG (50 nM, 20 min) or MTR(50 nM, 20 min), respectively.

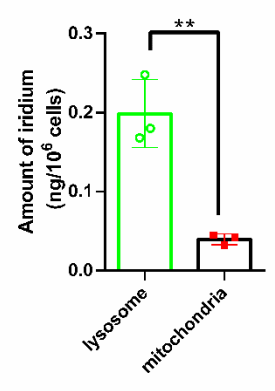

Fig. S25 ICP-MS assays for the distribution of **IrL** (30 μM) within different cellular compartments of EMT6 cells.

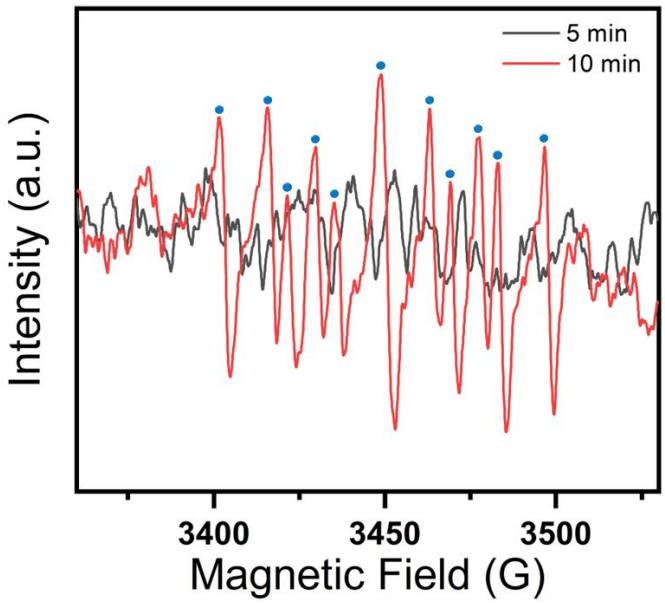

Fig. S26 EPR signals of NAD• radicals generated by **IrL** and trapped by CYPMPO at different times after light irradiation (390 nm, 45 mW cm^{-2}).

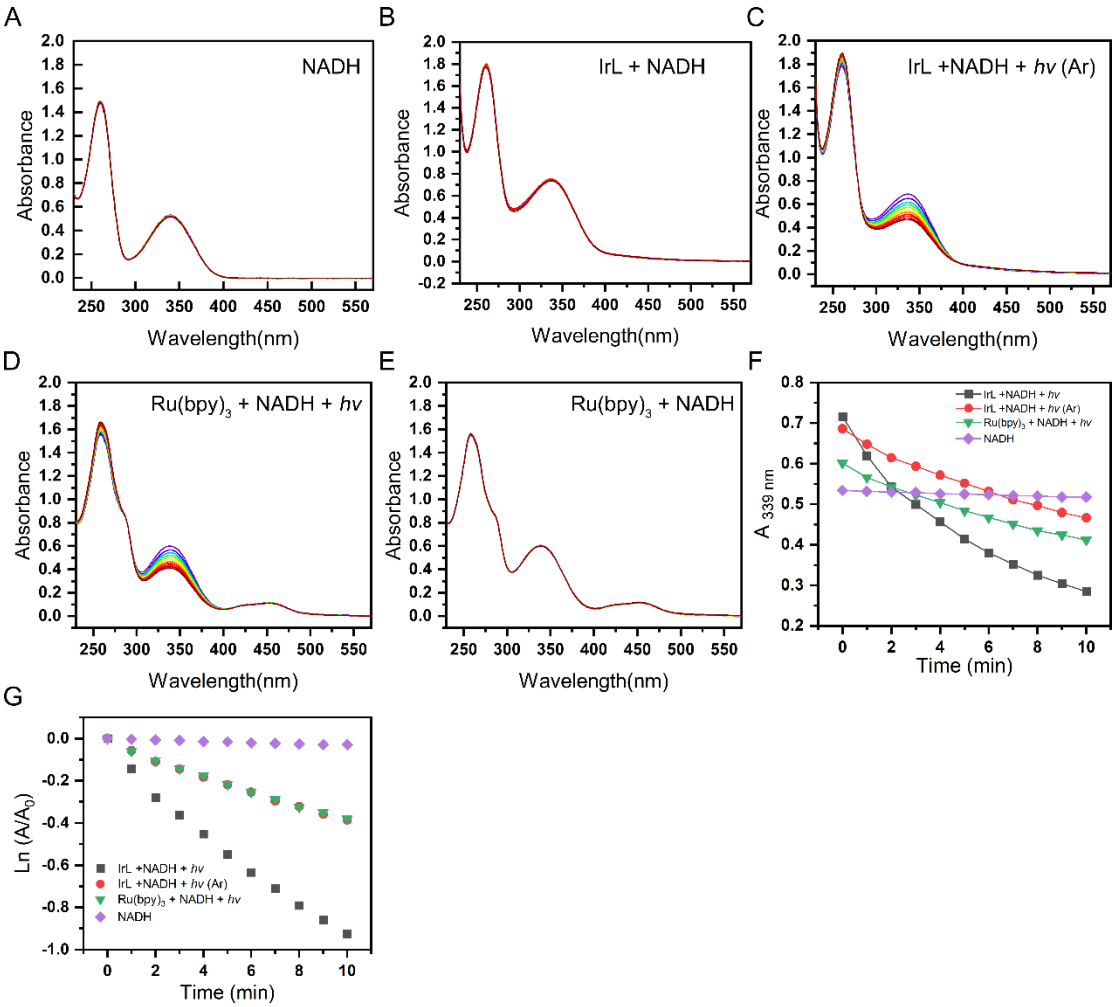

Fig. S27 Photocatalytic oxidation of NADH. (A) Only NADH. (B) **IrL** and NADH in H_2O. (C) **IrL** and NADH in H_2O degassed with Ar, light irradiation. (D) $[Ru(bpy)_3]Cl_2$ and NADH in H_2O, light irradiation. (E) $[Ru(bpy)_3]Cl_2$ and NADH in H_2O, no light irradiation. (F) The absorbance change of NADH at 339 nm at various time points. (G) Rate of decay of NADH at 339 nm under different conditions. Conditions: [**IrL**] = $[Ru(bpy)_3]Cl_2$ = 10 μM, [NADH] = 100 μM. Light irradiation = LED light (390 nm, 45 mW cm^{-2}).

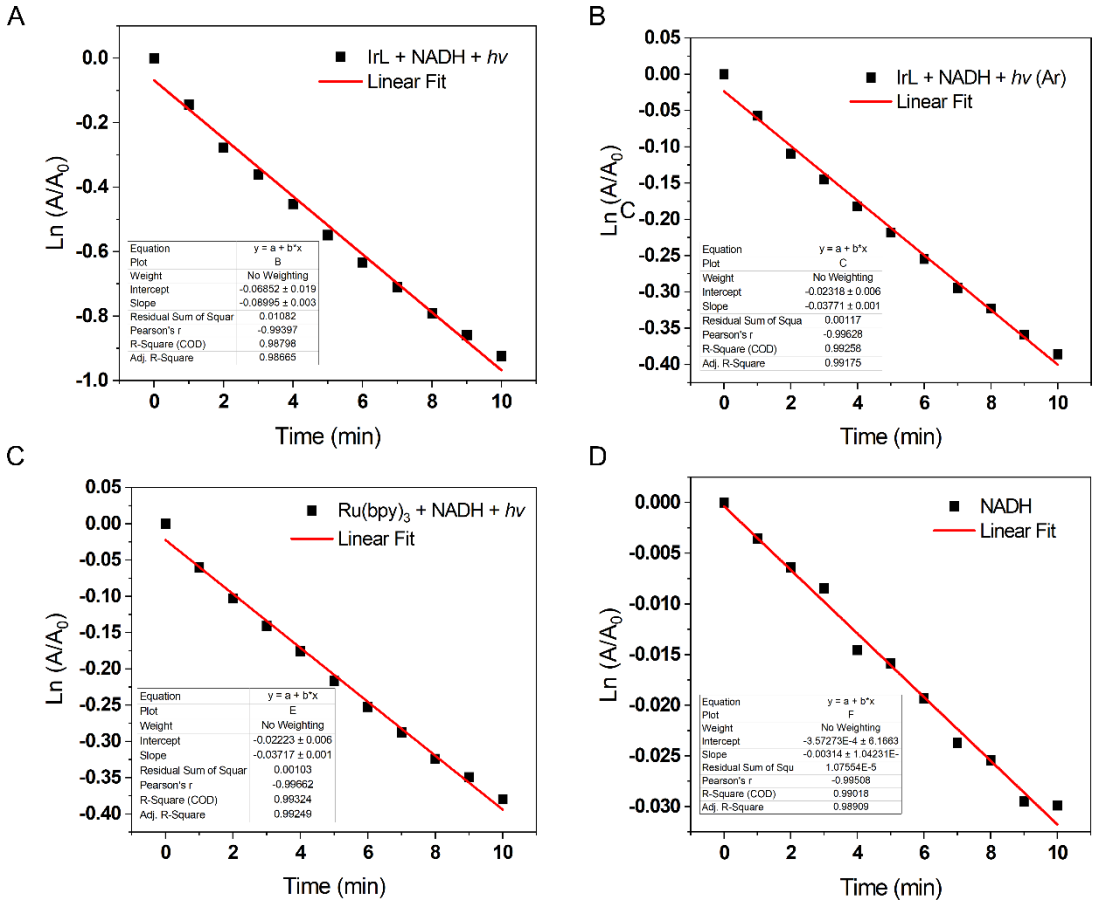

Fig. S28 Rate of decay of NADH at 339 nm under different conditions. (A) **IrL** and NADH in H_2O, light irradiation. (B) **IrL** and NADH in H_2O degassed with Ar, light irradiation. (C) $[Ru(bpy)_3]Cl_2$ and NADH in H_2O, light irradiation. (D)Only NADH. Conditions: [**IrL**] = $[Ru(bpy)_3]Cl_2$ = 10 μM, [NADH] = 100 μM. Light irradiation = LED light (390 nm, 45 mW cm^{-2}).

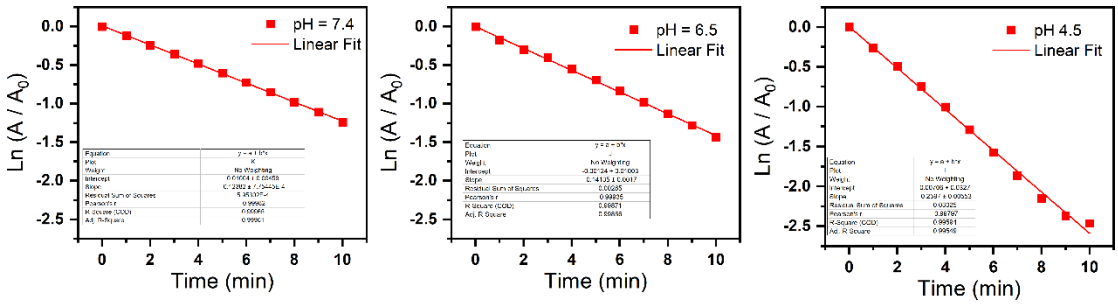

Fig. S29 Rate of decay of ABDA at 378 nm under different pH conditions.

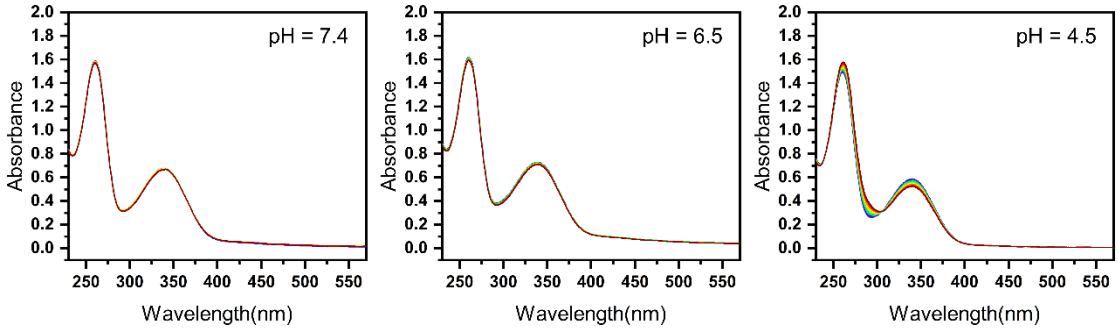

Fig. S30 Photocatalytic oxidation of NADH under acid conditions without light irradiation.

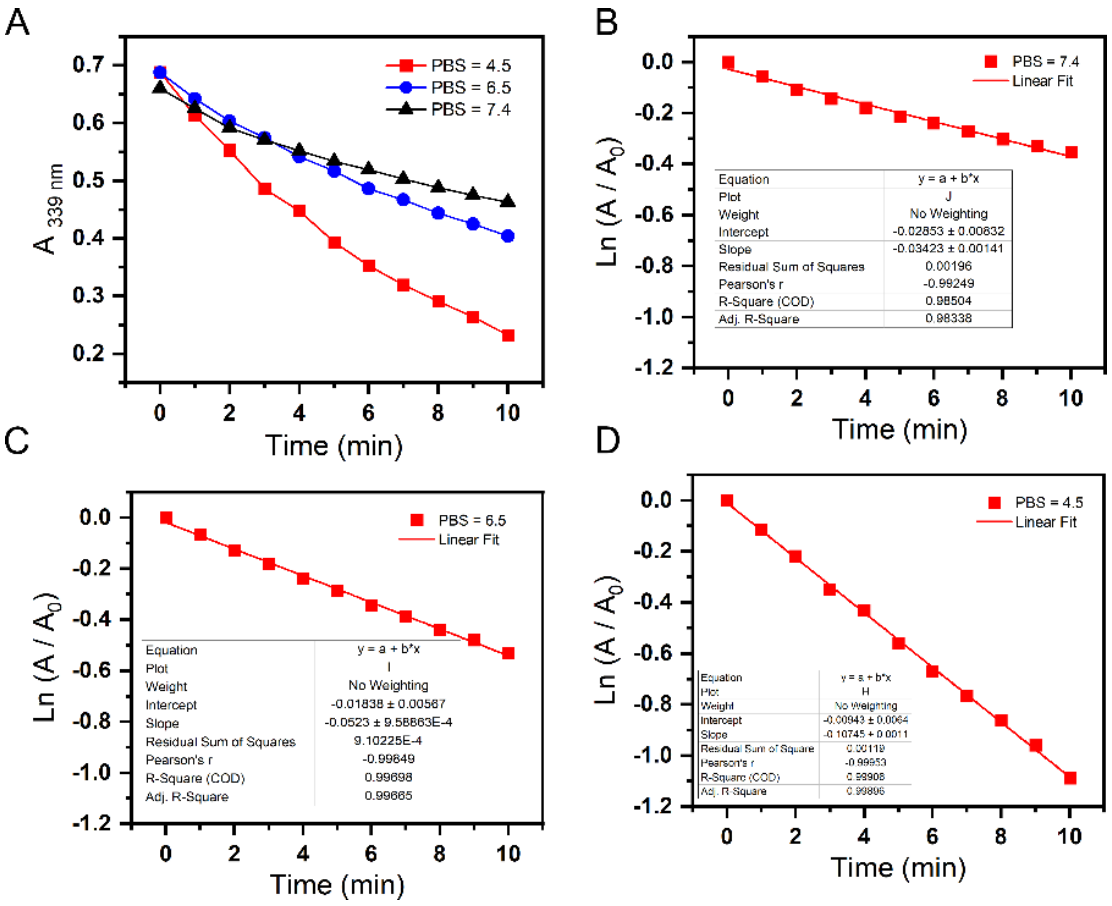

Fig. S31 Rate of decay of NADH at 339 nm under different pH conditions. (A) The absorbance change of NADH at 339 nm at different pH conditions. (B) pH = 7.4. (C) pH = 6.5. (D) pH = 4.5. Conditions: [**IrL**] = 10 μM, [NADH] = 100 μM. Light irradiation = LED light (390 nm, 45 mW cm^{-2}).

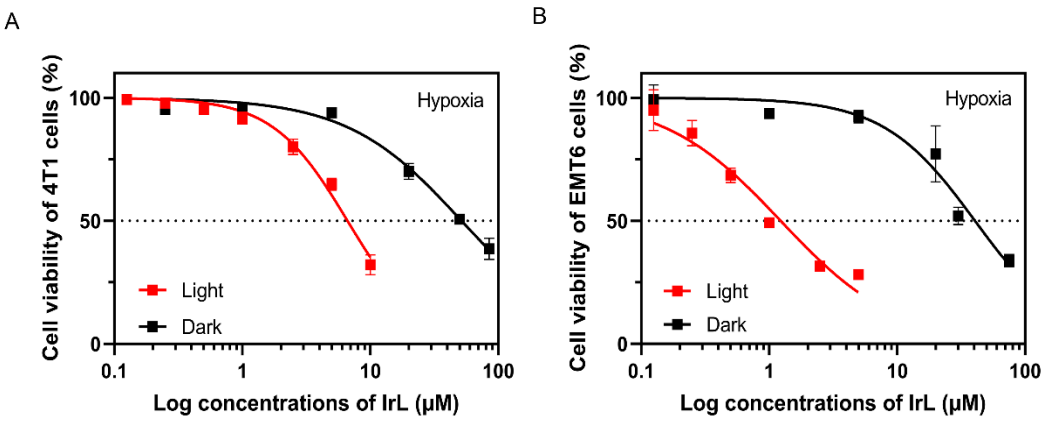

Fig. S32 Cell viability assessment. Dark- and photo-toxicity of 4T1 cells (A) and EMT6 cells (B) exposed to the **IrL** under hypoxia (5% oxygen) for 48 h using MTS assays.

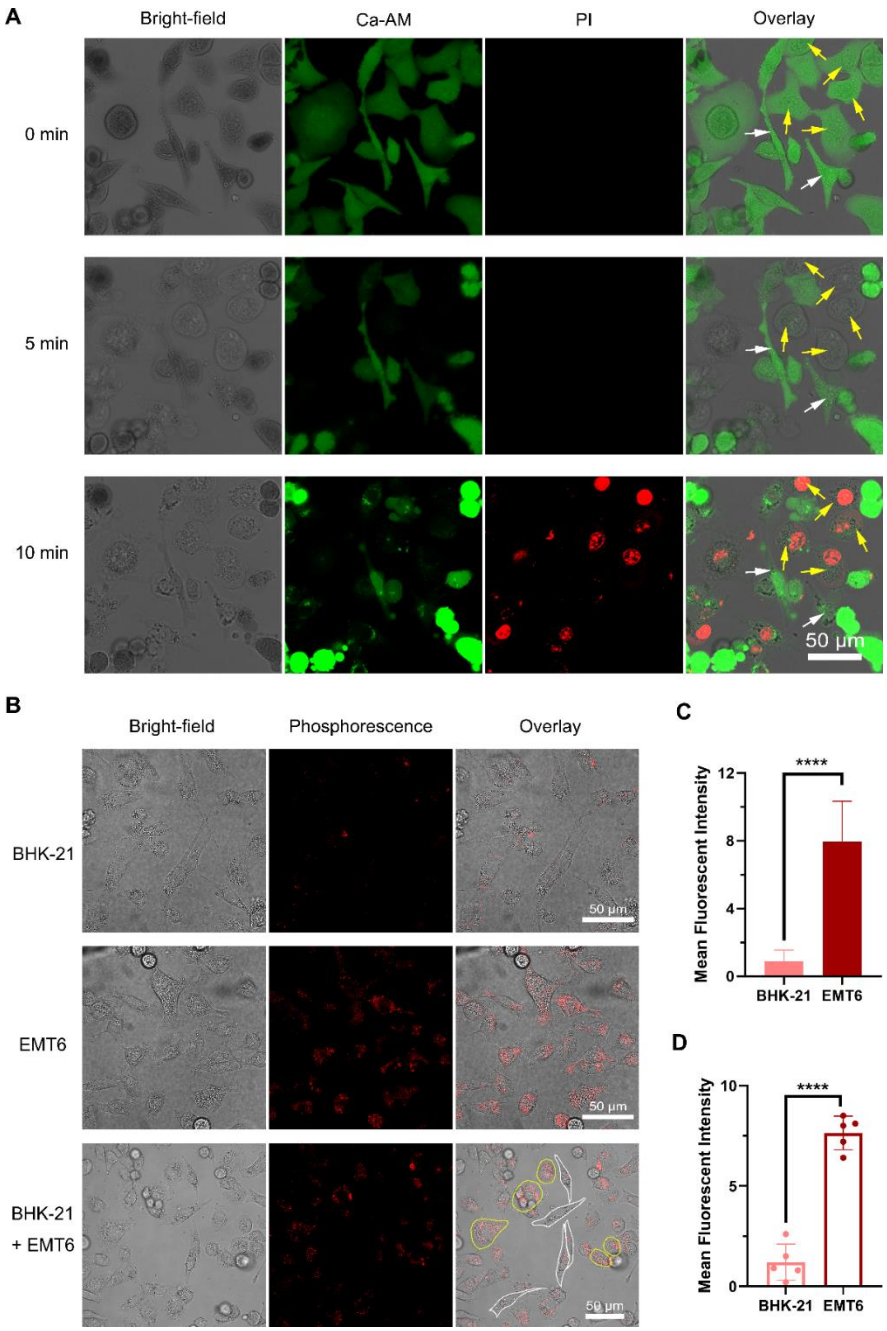

Fig. S33 Selectivity in killing cancer over normal cells. (A) **IrL**-mediated PDT in a EMT6/BHK-21 co-culture cell model as determined by Ca-AM/PI assay. Yellow arrows represent EMT6 cells, whereas white arrows represent BHK-21 cells. (B) Confocal images of the internalization of **IrL** by BHK-21 and EMT6 cells. The yellow outline represents EMT6 cells, whereas white outline represents BHK-21 cells. (C) Comparison of the phosphorescence intensity of **IrL** between the BHK-21 and EMT6 cells. (D) Comparison of the phosphorescence intensity of **IrL** in a EMT6/BHK-21 co-culture cell model.

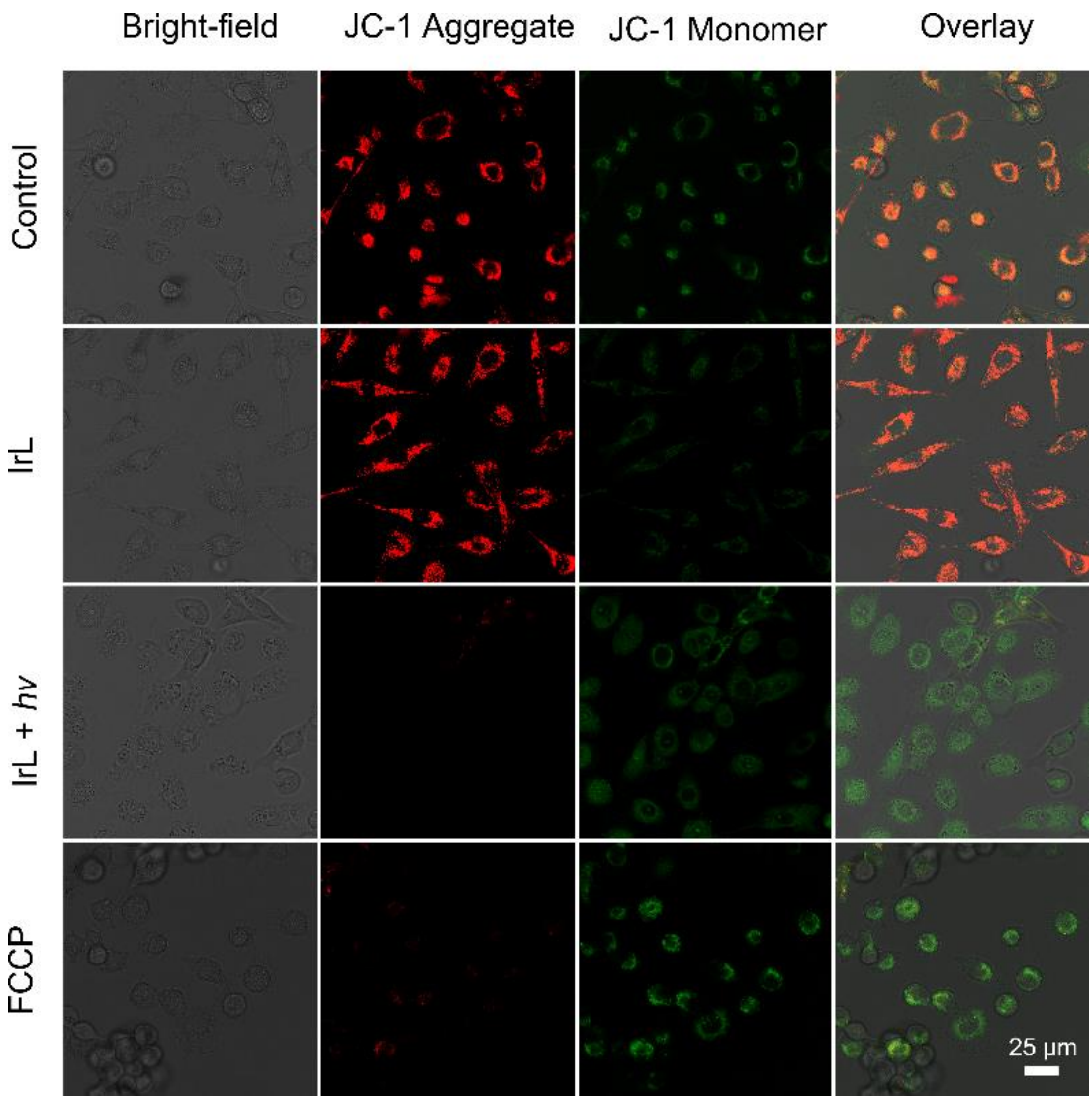

Fig. S34 Mitochondrial membrane potential of 4T1 cells was assessed using JC-1 staining. The cells were subjected to different incubation conditions: (A) Control (untreated), (B) **IrL** (30 μM, 4 h) incubation in the dark, (C) **IrL** (30 μM, 4 h) incubation with light treatment, (D) FCCP (10 μM) pretreatment for 60 minutes followed by **IrL** (30 μM) incubation with light treatment. Then the cells were incubated with JC-1 (5 μg/mL) at 37 °C for 20 min. Light irradiation = LED light (390 nm, 45 mW cm^{-2}, 20 min). Scale bar: 25 μm.

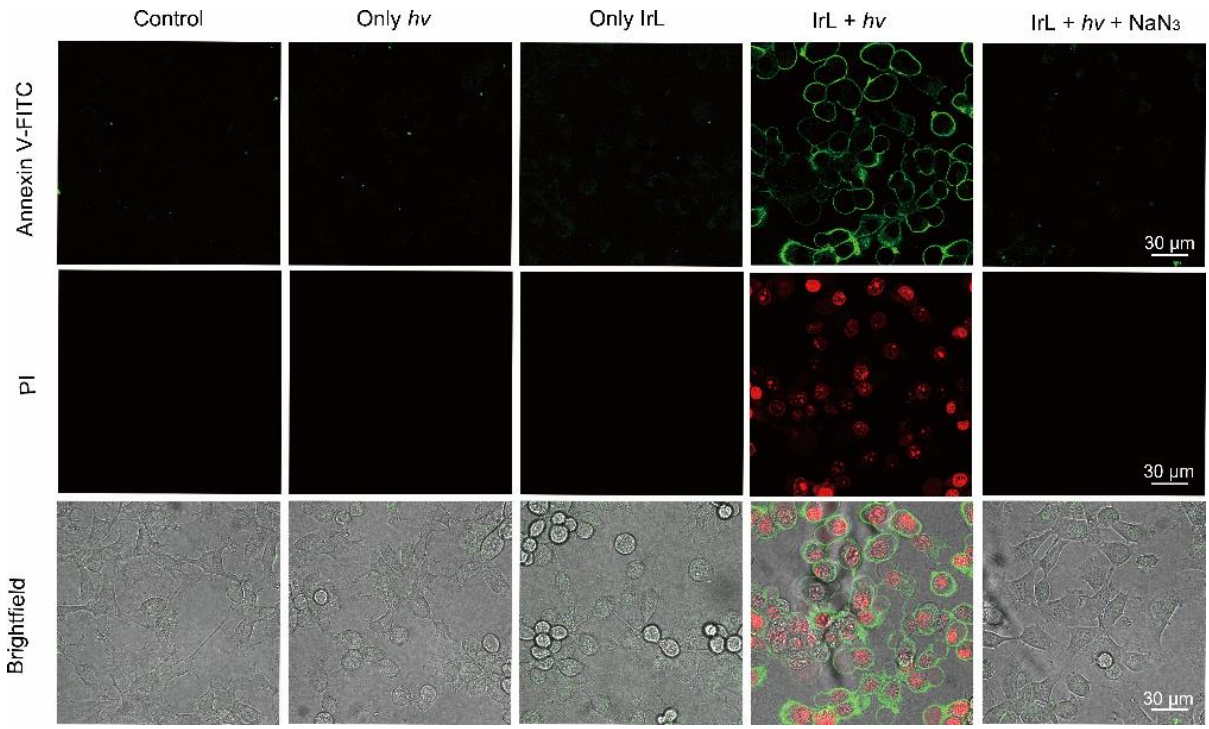

Fig. S35 Detection of apoptosis in 4T1 cells stained with Annexin V/ PI by confocal microscopy after PDT treatment with **IrL** (30 μM, 4 h) under 390 nm light and dark conditions.

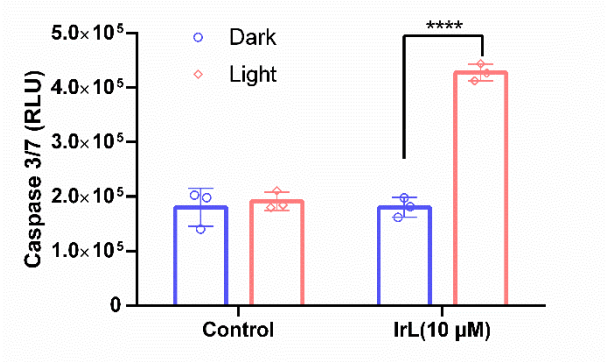

Fig. S36 Detection of caspase-3/7 activity in 4T1 cells after treated with **IrL** (10 μM, 4 h) in the absence or presence of light at the indicated concentrations. Light conditions: 390 nm (45 mW cm^{-2}) for 20 min.

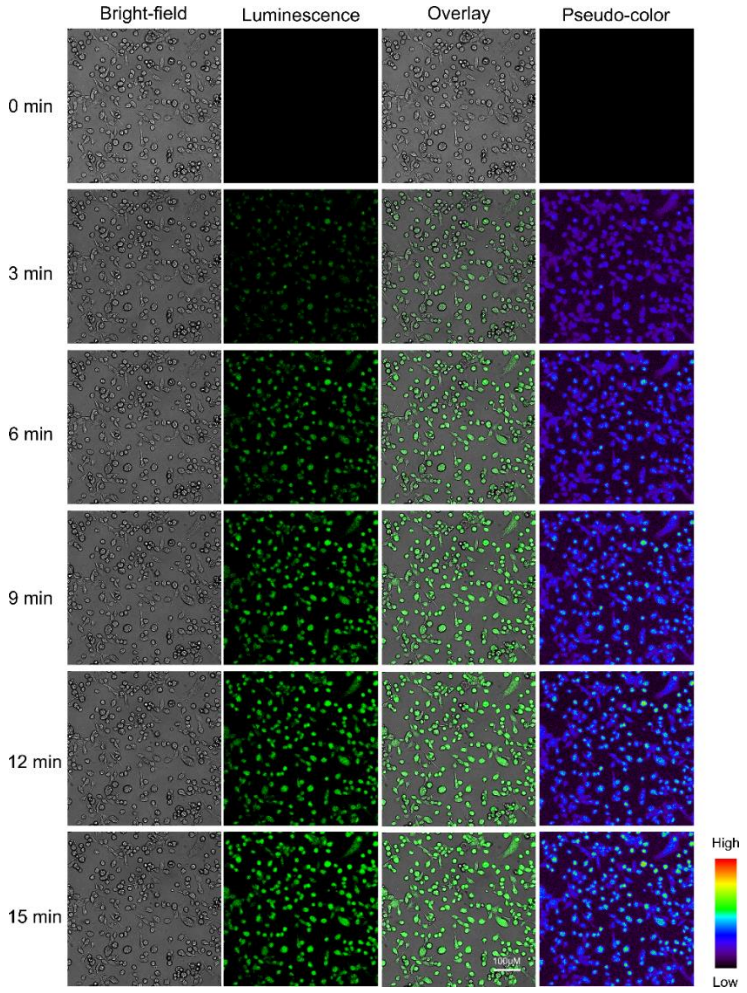

Fig. S37 Cellular ROS detection. 4T1 cells were treated with **IrL** (30 μM) for 4 h at 37°C, followed by further incubated with DCFH-DA (10 μM) for 20 min in the dark. Subsequently, the cells were irradiated with a 405 nm laser (0.11%) and images were acquired using a Leica *Stellaris* 5 confocal microscope.

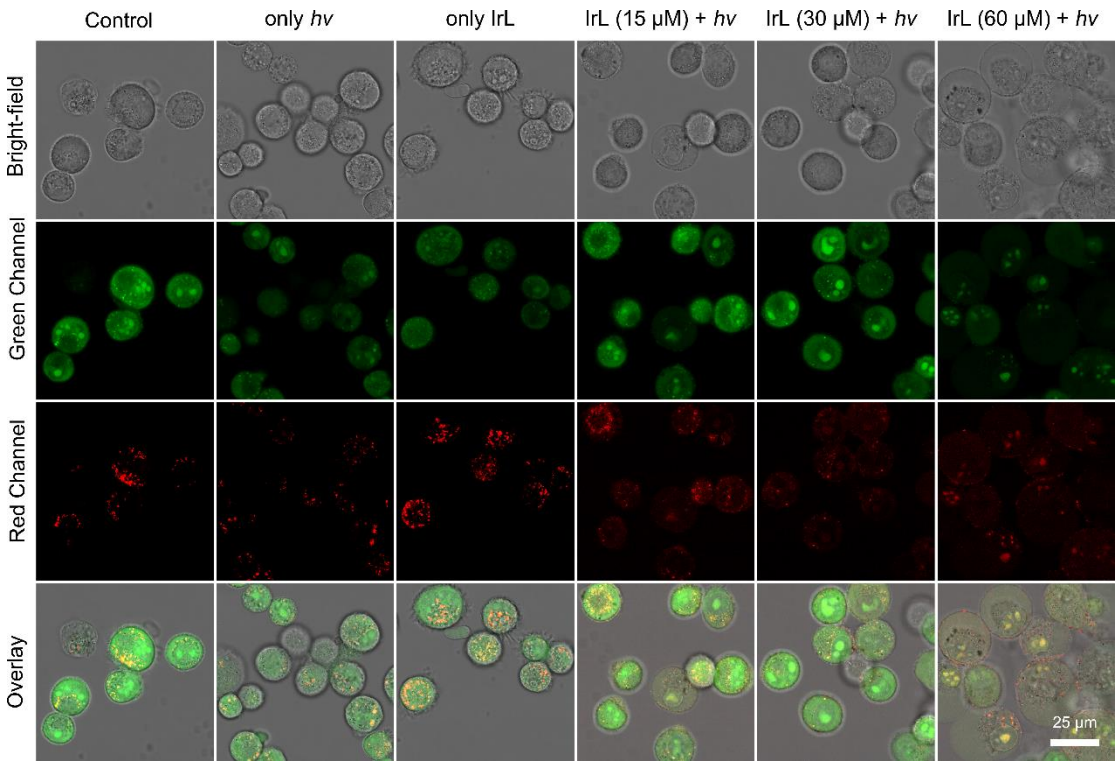

Fig. S38 AO staining under various conditions. (A) Control, (B) light treatment, (C) **IrL** (30 μM) dark treatment, (D) **IrL** (15 μM) with light treatment, (E) **IrL** (30 μM) with light treatment, and (F) **IrL** (60 μM) with light treatment. Scale bar: 25 μm.

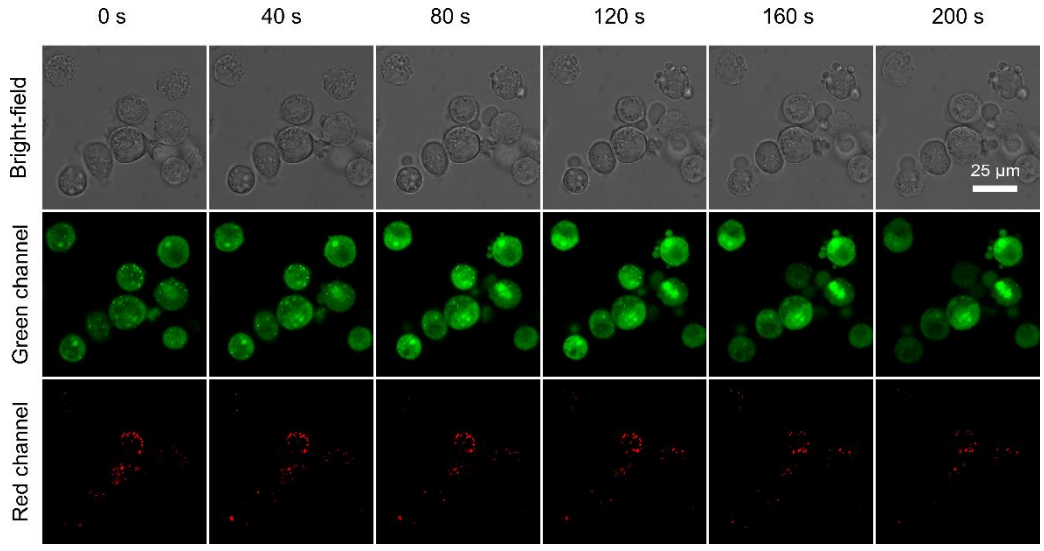

Fig. S39 Real-time monitoring of lysosomal disruption using AO staining. 4T1 cells were incubated with **IrL** (30 μM) for 4 h, followed by incubation with AO (5 μM) for 15 min. Subsequently, the cells were irradiated with a 405 nm laser (2%) and images were acquired using a Leica *Stellaris* 5 confocal microscope.

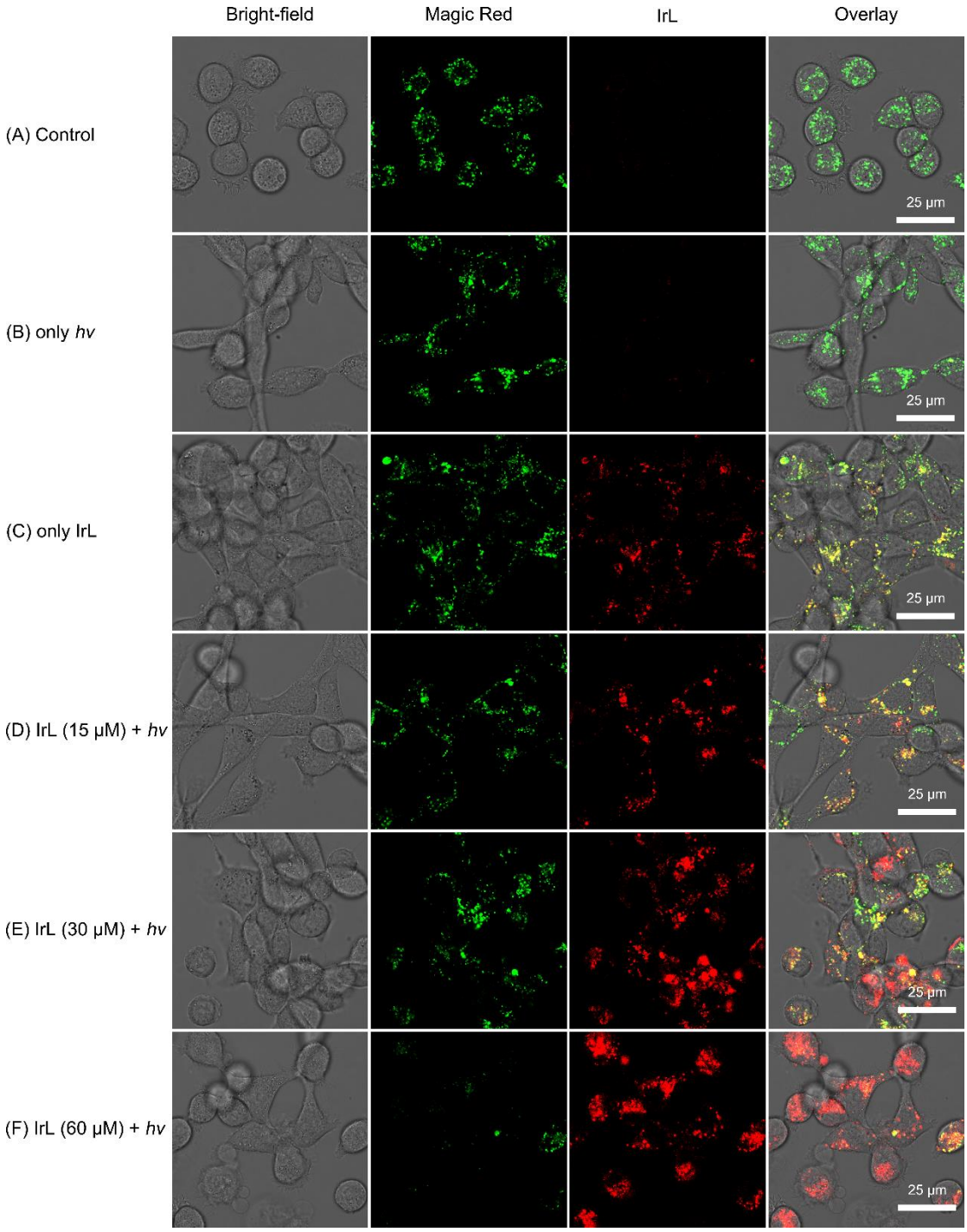

Fig. S40 Measurement of Cathepsin B activity under various conditions. Magic Red MR-$(RR)_2$ staining for assessing the release of cathepsin B from lysosomes in 4T1 cells caused by **IrL**-mediated PDT. 4T1 cells were treated with (A) dark treatment alone, (B) light treatment alone, (C) **IrL** (30 μM) dark treatment, (D) **IrL** (15 μM) with light treatment, (E) **IrL** (30 μM) with light treatment, (F) **IrL** (60 μM) with light treatment. Scale bar: 25 μm.

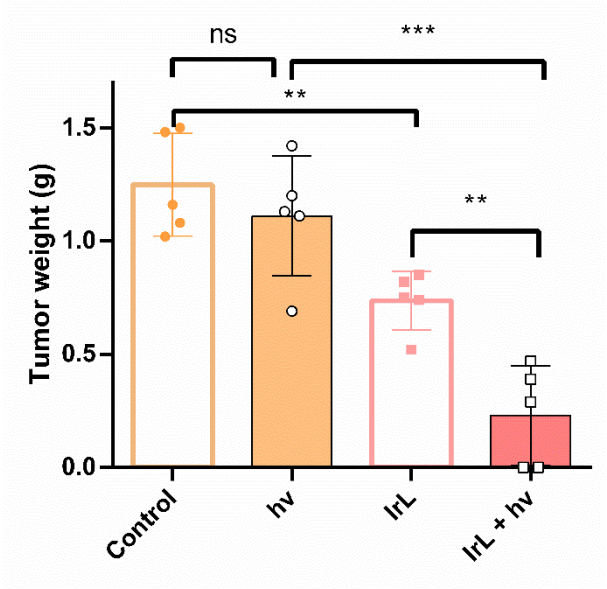

Fig. S41 Average tumor weights of mice at 14 day post various treatments.

Supporting tables

Table S1. The original data and calculated values for phosphorescence quantum yields.

No.	n_u	n_s	A_u	A_s	D_u	D_s	Φ_s	$\boldsymbol{\Phi_u}$
1	1.344	1.344	0.07644	0.03719	3.47E+08	5.10E+08	0.028	**0.009**
2	1.344	1.344	0.08635	0.03629	3.54E+08	5.20E+08	0.028	**0.008**
3	1.344	1.344	0.05486	0.03773	3.55E+08	5.09E+08	0.028	**0.013**
$\Phi_u = (\Phi_{u1} + \Phi_{u2} + \Phi_{u3})/3 = (0.009 + 0.008 + 0.013)/3 = 0.010$ SD = 0.003								

SD = Standard Deviation.

Table S2. The original data and calculated values for lipid–water distribution coefficient (log $P_{o/w}$).

No.	A_{278}	C_w	$P_{o/w}$	log $P_{o/w}$
1	0.055	1.141	16.534	1.218
2	0.065	1.459	12.710	1.104
3	0.078	1.872	9.681	0.986
$\log P_{o/w} = (\log P_{o/w\,1} + \log P_{o/w\,2} + \log P_{o/w\,3})/3 = (1.218 + 1.104 + 0.986)/3 = 1.10$ SD = 0.12				

SD = Standard Deviation.

Table S3. DFT optimized coordinates for **IrL** in the ground state.

Number	Atom	Coordinates		
		X	Y	Z
1	N	-0.179845	-0.803647	0.948928
2	N	-0.187426	0.927488	-1.080418
3	C	2.231480	1.023462	-1.187111
4	C	-2.804855	-2.702600	-0.729824
5	C	-2.880079	2.613678	0.791397

6	C	3.431419	0.525774	-0.606552
7	C	2.240379	-0.877649	1.019088
8	C	-0.258092	1.795499	-2.083335
9	H	-1.253539	2.078317	-2.408895
10	C	3.454727	-0.384682	0.446731
11	C	2.177300	-1.791474	2.083208
12	H	3.096806	-2.168343	2.518987
13	C	0.941185	-2.186629	2.548966
14	H	0.845622	-2.889807	3.368816
15	C	-3.902584	-0.637711	2.178327
16	H	-3.692048	0.333293	2.619094
17	C	-3.529804	-2.305497	0.482360
18	C	1.031441	-0.401212	0.469615
19	C	-0.218427	-1.672261	1.958207
20	H	-1.205333	-1.956609	2.303526
21	C	1.027241	0.537796	-0.621458
22	C	2.133020	1.935942	-2.254121
23	H	3.026090	2.333043	-2.726053
24	C	-1.119560	1.969017	2.299068
25	H	-0.357448	1.269735	2.636157
26	C	0.885321	2.320644	-2.697683
27	H	0.774610	3.023267	-3.515961
28	C	-3.670713	2.247356	-0.380336
29	C	-4.846936	-1.465828	2.784294
30	H	-5.358891	-1.131500	3.683864
31	C	-5.139295	-2.718311	2.243359
32	H	-5.875323	-3.364419	2.713326
33	C	-2.203412	-4.184701	-2.534867
34	H	-2.311750	-5.133586	-3.051474
35	C	-1.220936	-2.024985	-2.308428
36	H	-0.551534	-1.234659	-2.632610
37	C	-1.299747	3.156778	3.007252
38	H	-0.678245	3.365608	3.875155
39	C	-1.319935	-3.216688	-3.008103
40	H	-0.719481	-3.376040	-3.896755
41	C	-2.270913	4.079417	2.612365
42	H	-2.409287	5.003556	3.166195
43	C	-3.995774	0.597043	-2.012007
44	H	-3.679725	-0.366902	-2.392653
45	C	-5.370667	2.546930	-2.066035
46	H	-6.166607	3.138831	-2.507306
47	C	-5.015714	1.314816	-2.611998
48	H	-5.516123	0.909945	-3.484362
49	N	4.748329	0.767583	-0.883643
50	C	5.500110	0.019574	-0.016232
51	C	6.957421	0.011659	-0.002113
52	C	7.619491	-0.732822	0.984177
53	C	7.729461	0.716327	-0.937589
54	C	9.003318	-0.774083	1.039903
55	H	7.029944	-1.281084	1.711918
56	C	9.113581	0.681542	-0.889191

57	H	7.261432	1.300465	-1.724973
58	C	9.760671	-0.064546	0.101292
59	H	9.500192	-1.356154	1.812553
60	H	9.709692	1.226197	-1.614534
61	N	-1.939734	-1.771978	-1.206118
62	O	11.111048	-0.061555	0.099420
63	H	11.438576	-0.610618	0.827596
64	H	5.103696	1.402016	-1.583529
65	N	4.734165	-0.689180	0.800654
66	C	-4.695184	3.010158	-0.948356
67	H	-4.958386	3.965503	-0.508928
68	C	-3.060636	3.807294	1.503095
69	H	-3.814822	4.528125	1.197775
70	C	-4.480611	-3.134842	1.094307
71	H	-4.714670	-4.110458	0.676804
72	C	-2.946355	-3.926360	-1.393051
73	H	-3.634465	-4.673425	-1.014703
74	Ir	-1.816299	0.024386	0.003757
75	C	-3.216448	-1.028068	1.018837
76	C	-1.902783	1.661982	1.177486
77	N	-3.337058	1.046874	-0.931310

Table S4. DFT optimized coordinates for **IrLH** in the ground state.

Number	Atom	Coordinates		
		X	Y	Z
1	N	-0.212615	-0.800098	0.974058
2	N	-0.176865	0.882747	-1.087580
3	C	2.236950	0.958926	-1.167429
4	C	-2.867845	-2.698582	-0.674498
5	C	-2.864280	2.649415	0.711953
6	C	3.426499	0.459076	-0.560959
7	C	2.202216	-0.906210	1.086858
8	C	-0.223609	1.731268	-2.108588
9	H	-1.211694	2.016416	-2.453731
10	C	3.409069	-0.421571	0.500538
11	C	2.112886	-1.794313	2.171226
12	H	3.002955	-2.183948	2.653538
13	C	0.863357	-2.162258	2.621634
14	H	0.747827	-2.844722	3.455630
15	C	-3.931807	-0.543498	2.180787
16	H	-3.704767	0.434113	2.597718
17	C	-3.587053	-2.259434	0.526409
18	C	1.009430	-0.424034	0.505616
19	C	-0.278020	-1.647255	2.000539
20	H	-1.273841	-1.911502	2.335841
21	C	1.028092	0.493687	-0.605601
22	C	2.169795	1.848267	-2.253205
23	H	3.070731	2.226675	-2.724400
24	C	-1.124793	2.019845	2.250125
25	H	-0.376191	1.319448	2.614020
26	C	0.930816	2.234201	-2.719520

27	H	0.836545	2.920073	-3.553468
28	C	-3.651990	2.262754	-0.455134
29	C	-4.890831	-1.340182	2.805771
30	H	-5.397390	-0.974915	3.696194
31	C	-5.204321	-2.600145	2.295412
32	H	-5.951596	-3.221609	2.780482
33	C	-2.295592	-4.232604	-2.444984
34	H	-2.423600	-5.190015	-2.940828
35	C	-1.267944	-2.089657	-2.265101
36	H	-0.581774	-1.321784	-2.607490
37	C	-1.293907	3.228133	2.926015
38	H	-0.676870	3.450286	3.793654
39	C	-1.391264	-3.294242	-2.938038
40	H	-0.793554	-3.485624	-3.822151
41	C	-2.248567	4.153217	2.499096
42	H	-2.378444	5.093219	3.027579
43	C	-3.988276	0.573962	-2.045419
44	H	-3.682936	-0.403462	-2.398951
45	C	-5.336869	2.539563	-2.159315
46	H	-6.122213	3.129765	-2.621248
47	C	-4.994695	1.289153	-2.670461
48	H	-5.494845	0.867960	-3.535142
49	N	4.751080	0.699073	-0.845835
50	C	5.540136	0.003857	-0.008345
51	C	6.981482	-0.006561	0.006282
52	C	7.677931	-0.350280	1.176399
53	C	7.708978	0.326760	-1.150608
54	C	9.060138	-0.363156	1.192789
55	H	7.145883	-0.579564	2.094978
56	C	9.089024	0.315523	-1.137573
57	H	7.198540	0.565620	-2.079043
58	C	9.776097	-0.030476	0.034874
59	H	9.588461	-0.620582	2.106364
60	H	9.656493	0.560578	-2.029016
61	N	-1.982479	-1.797113	-1.169507
62	O	11.115857	-0.024075	-0.016657
63	H	11.487028	-0.282633	0.841400
64	H	5.102722	1.357344	-1.528542
65	N	4.724130	-0.680221	0.812378
66	H	5.052656	-1.343697	1.501552
67	C	-4.662510	3.023465	-1.049737
68	H	-4.915991	3.993287	-0.637218
69	C	-3.033676	3.863270	1.390991
70	H	-3.775584	4.585946	1.061312
71	C	-4.552370	-3.056677	1.157802
72	H	-4.802716	-4.038256	0.764643
73	C	-3.034396	-3.933331	-1.310557
74	H	-3.739315	-4.656592	-0.917360
75	Ir	-1.830837	0.026608	-0.002519
76	C	-3.253036	-0.975299	1.032313
77	N	-3.330782	1.044000	-0.972383

78	C	-1.902942	1.695971	1.130478

Table S5. Molecular Orbital Compositions of **IrL** under TD-DFT Singlet Excitation Calculation (Excitation Transition Study).

Orbital	Energy(eV)	MO contribution (%)		
		Ir	ppy	L
LUMO+10	-0.0485	5.66	78.41	15.90
LUMO+9	-0.1493	1.42	10.97	87.61
LUMO+8	-0.5107	1.15	4.30	94.54
LUMO+7	-0.5526	0.05	0.04	99.90
LUMO+6	-1.0869	1.47	96.90	1.63
LUMO+5	-1.2922	1.53	83.31	15.15
LUMO+4	-1.5541	0.85	16.14	83.01
LUMO+3	-1.7197	4.01	93.92	2.08
LUMO+2	-1.8138	3.33	93.96	2.71
LUMO+1	-2.0868	1.17	1.58	97.26
LUMO	-2.4942	3.73	2.20	94.07
HOMO	-6.1969	11.02	17.29	71.69
HOMO–1	-6.2604	24.67	46.02	29.31
HOMO–2	-6.4123	27.60	67.35	5.05
HOMO–3	-6.9043	22.82	71.71	5.47
HOMO–4	-6.9990	21.84	66.59	11.56
HOMO–5	-7.0699	23.66	68.07	8.28
HOMO–6	-7.5028	2.96	9.98	87.07
HOMO–7	-7.6568	3.86	3.32	92.82
HOMO–8	-7.7796	0.60	1.20	98.19
HOMO–9	-7.8108	22.77	69.03	8.19
HOMO–10	-7.9130	24.93	52.42	22.65

Table S6. TD-DFT Calculated Singlet Absorption Data for **IrL**.

State	Transition	Contribution%	*E*,nm (eV)	o.s.	Assignment
S1	HOMO–1→LUMO	53.6	433 (2.86)	0.0366	^{1}MLCT/^{1}LLCT/^{1}ILCT
S2	HOMO→LUMO	48.8	412 (3.01)	0.1075	^{1}MLCT/^{1}LLCT/^{1}ILCT
S3	HOMO–2→LUMO	86.4	403 (3.08)	0.0032	^{1}MLCT/^{1}LLCT
S4	HOMO–1→LUMO+1	67.7	365 (3.39)	0.0168	^{1}MLCT/^{1}LLCT/^{1}ILCT
S5	HOMO–1→LUMO+2	56.7	359 (3.46)	0.0323	^{1}MLCT/^{1}LLCT
S6	HOMO→LUMO+1	67.2	355 (3.49)	0.1557	^{1}MLCT/^{1}LLCT/^{1}ILCT
S7	HOMO–3→LUMO	45.2	349 (3.55)	0.0557	^{1}MLCT/^{1}LLCT
S8	HOMO–2→LUMO+1	82.6	345 (3.59)	0.0541	^{1}MLCT/^{1}LLCT
S9	HOMO–1→LUMO+3	47.5	343 (3.62)	0.0359	^{1}MLCT/^{1}LLCT
S10	HOMO–2→LUMO+2	71.0	332 (3.73)	0.0705	^{1}MLCT/^{1}LLCT
S11	HOMO–4→LUMO	52.9	328 (3.78)	0.0417	^{1}MLCT/^{1}LLCT/^{1}ILCT
S12	HOMO–2→LUMO+3	64.5	324 (3.83)	0.0298	^{1}MLCT/^{1}ILCT
S13	HOMO–5→LUMO	69.3	320 (3.87)	0.0005	^{1}MLCT/^{1}LLCT
S14	HOMO→LUMO+2	50.9	316 (3.93)	0.0763	^{1}MLCT/^{1}LLCT
S15	HOMO→LUMO+4	50.7	312 (3.97)	0.1407	^{1}MLCT/^{1}LLCT/^{1}ILCT

Table S7. Calculated molecular orbitals of **IrL** under excited states TD-DFT (Excitation Transition).

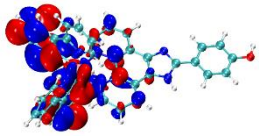	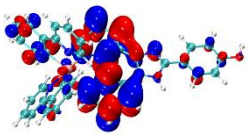	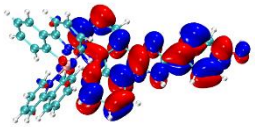
LUMO+10	**LUMO+9**	**LUMO+8**
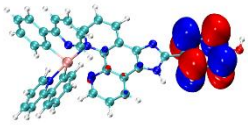	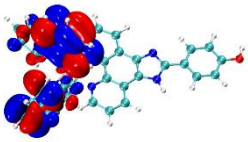	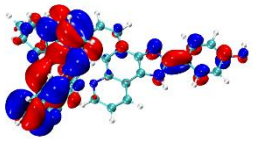
LUMO+7	**LUMO+6**	**LUMO+5**
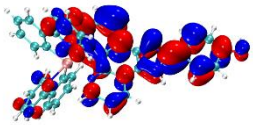	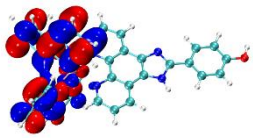	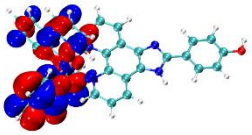
LUMO+4	**LUMO+3**	**LUMO+2**
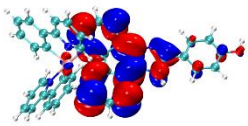	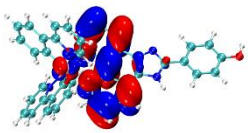	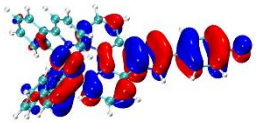
LUMO+1	**LUMO**	**HOMO**
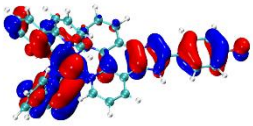	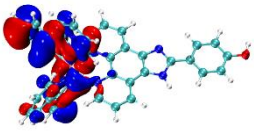	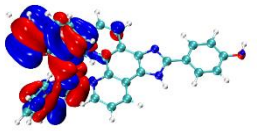
HOMO–1	**HOMO–2**	**HOMO–3**
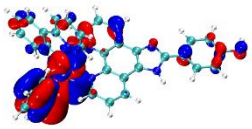		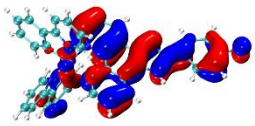
HOMO–4	**HOMO–5**	**HOMO–6**

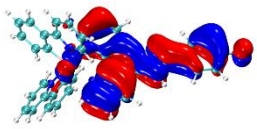	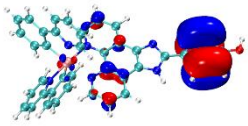	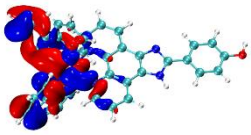
HOMO–7	**HOMO–8**	**HOMO–9**
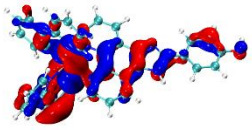		
HOMO–10		

Table S8. Molecular Orbital Compositions of **IrLH** under TD-DFT Singlet Excitation Calculation (Excitation Transition Study).

Orbital	Energy(eV)	MO contribution (%)		
		Ir	bpy	L
LUMO+10	-0.1361	7.51	85.24	7.23
LUMO+9	-0.5553	1.37	1.56	97.07
LUMO+8	-0.9849	0.02	0.04	99.94
LUMO+7	-1.0887	1.84	29.90	68.26
LUMO+6	-1.1492	1.37	84.93	13.71
LUMO+5	-1.4161	1.27	81.94	16.79
LUMO+4	-1.7803	3.90	94.92	1.18
LUMO+3	-1.8723	3.30	94.84	1.86
LUMO+2	-2.3813	0.86	1.04	98.11
LUMO+1	-2.5697	1.07	1.07	97.85
LUMO	-2.8344	3.71	2.00	94.29
HOMO	-6.3446	32.14	63.93	3.93
HOMO–1	-6.5004	26.41	69.72	3.87
HOMO–2	-6.9491	14.89	13.12	71.99
HOMO–3	-6.9835	7.21	86.17	6.62
HOMO–4	-7.1052	5.13	84.43	10.44
HOMO–5	-7.2203	45.01	26.86	28.12
HOMO–6	-7.8840	19.66	55.96	24.38
HOMO–7	-7.9151	24.50	60.79	14.71
HOMO–8	-8.1509	14.50	47.37	38.14
HOMO–9	-8.2033	10.62	25.01	64.37
HOMO–10	-8.2258	0.91	2.27	96.82

Table S9. TD-DFT Calculated Singlet Absorption Data for **IrLH**.

State	Transition	Contribution%	*E*,nm (eV)	o.s.	Assignment
S1	HOMO→LUMO	95.4	470 (2.64)	0.0165	^{1}MLCT/^{1}LLCT
S2	HOMO–1→LUMO	95.0	438 (2.83)	0.0123	^{1}MLCT/^{1}LLCT
S3	HOMO→LUMO+1	96.4	410 (3.02)	0.0060	^{1}MLCT/^{1}LLCT
S4	HOMO–1→LUMO+1	96.8	388 (3.20)	0.0025	^{1}MLCT/^{1}LLCT

S5	HOMO–2→LUMO	61.9	377 (3.29)	0.2211	^{1}MLCT/^{1}LLCT/^{1}ILCT
S6	HOMO→LUMO+2	85.8	361 (3.44)	0.0064	^{1}MLCT/^{1}LLCT
S7	HOMO–3→LUMO	79.8	358 (3.46)	0.0531	^{1}LLCT
S8	HOMO→LUMO+3	82.6	353 (3.51)	0.0302	^{1}MLCT
S9	HOMO–4→LUMO	74.4	345 (3.59)	0.0013	^{1}LLCT
S10	HOMO–1→LUMO+2	84.1	343 (3.62)	0.0062	^{1}MLCT/^{1}LLCT
S11	HOMO–5→LUMO	61.7	342 (3.62)	0.0066	^{1}MLCT/^{1}LLCT/^{1}ILCT
S12	HOMO→LUMO+4	73.1	338 (3.66)	0.0286	^{1}MLCT
S13	HOMO–2→LUMO+1	58.0	336 (3.69)	0.0904	^{1}MLCT/^{1}LLCT/^{1}ILCT
S14	HOMO–1→LUMO+3	73.3	329 (3.77)	0.0573	^{1}MLCT
S15	HOMO–3→LUMO+1	73.5	327 (3.79)	0.0219	^{1}LLCT

Table S10. Calculated molecular orbitals of **IrLH** under excited states TD-DFT (Excitation Transition).

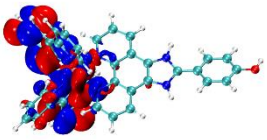	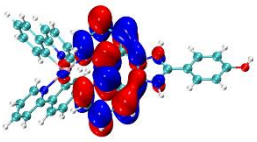	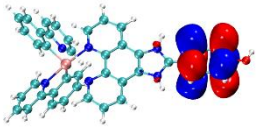
LUMO+10	**LUMO+9**	**LUMO+8**
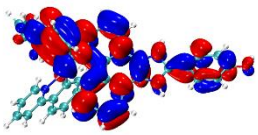	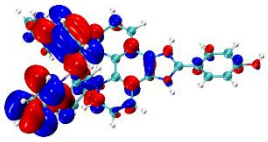	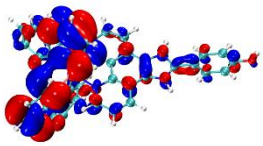
LUMO+7	**LUMO+6**	**LUMO+5**
	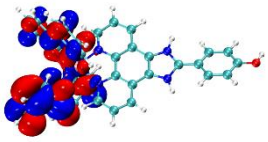	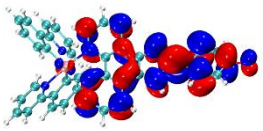
LUMO+4	**LUMO+3**	**LUMO+2**
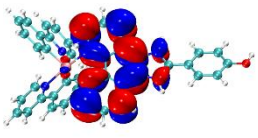	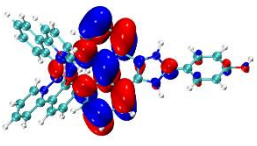	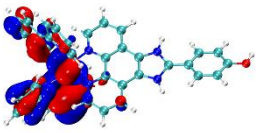
LUMO+1	**LUMO**	**HOMO**

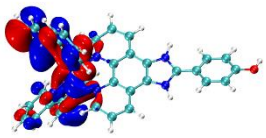	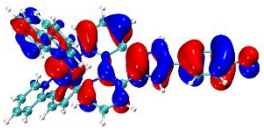	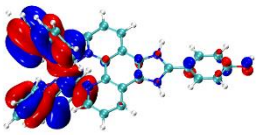
HOMO–1	**HOMO–2**	**HOMO–3**
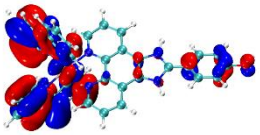	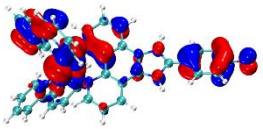	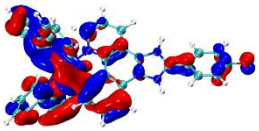
HOMO–4	**HOMO–5**	**HOMO–6**
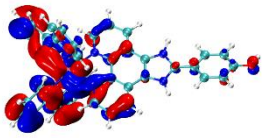	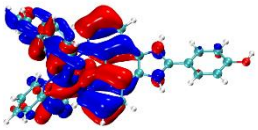	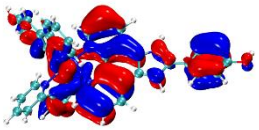
HOMO–7	**HOMO–8**	**HOMO–9**
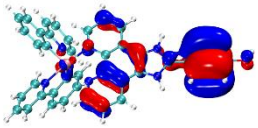		
HOMO–10		

Table S11. Molecular Orbital Compositions of **IrL** under TD-DFT Triplet Excitation Calculation (Emission Transition Study).

Orbital	Energy(eV)	MO contribution (%)		
		Ir	bpy	L
LUMO+10	-0.0353	5.36	77.09	17.51
LUMO+9	-0.1580	1.38	12.21	86.41
LUMO+8	-0.4542	1.35	5.25	93.39
LUMO+7	-0.5056	0.05	0.03	99.91
LUMO+6	-1.0882	1.45	97.06	1.48
LUMO+5	-1.2974	1.51	88.24	10.25
LUMO+4	-1.5782	0.73	11.37	87.90
LUMO+3	-1.7173	3.94	93.85	2.21
LUMO+2	-1.8077	3.35	93.88	2.77
LUMO+1	-2.0737	1.16	1.41	97.43
LUMO	-2.7464	4.23	2.26	93.51

HOMO	-5.9910	1.80	1.57	96.62
HOMO–1	-6.2335	32.77	61.22	6.00
HOMO–2	-6.4100	27.60	68.34	4.06
HOMO–3	-6.8983	24.10	68.78	7.13
HOMO–4	-6.9928	21.52	66.00	12.47
HOMO–5	-7.0593	20.38	70.64	8.98
HOMO–6	-7.4952	2.70	10.52	86.78
HOMO–7	-7.6341	5.40	3.48	91.12
HOMO–8	-7.8262	23.40	67.55	9.06
HOMO–9	-7.8389	1.49	3.86	94.64
HOMO–10	-7.9478	23.68	51.66	24.66

Table S12. TD-DFT Excitation Calculation for Emission for **IrL**.

State	Transition	Contribution%	*E*,nm (eV)	o.s.	Assignment
T1	HOMO→LUMO	82.5	586 (2.12)	0.0000	^{3}ILCT
T2	HOMO→LUMO+1	41.9	533 (2.32)	0.0000	^{3}ILCT
T3	HOMO–1→LUMO	59.7	487 (2.55)	0.0000	^{3}MLCT/^{3}LLCT
T4	HOMO→LUMO+4	34.8	457 (2.71)	0.0000	^{3}ILCT
T5	HOMO–2→LUMO	90.4	450 (2.76)	0.0000	^{3}MLCT/^{3}LLCT
T6	HOMO–1→LUMO+2	47.1	446 (2.78)	0.0000	^{3}MLCT
T7	HOMO–2→LUMO+3	29.6	436 (2.85)	0.0000	^{3}MLCT
T8	HOMO→LUMO+4	26.5	415 (2.99)	0.0000	^{3}ILCT

Table S13. Calculated molecular orbitals of **IrL** under excited states TD-DFT (Emission Transition).

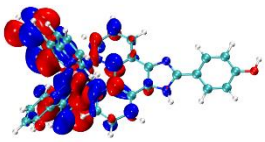	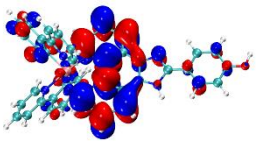	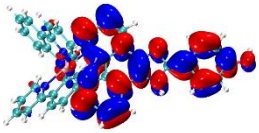
LUMO+10	**LUMO+9**	**LUMO+8**
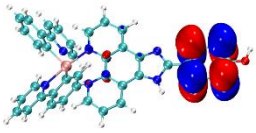	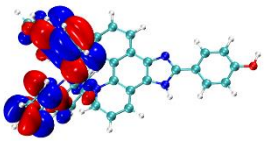	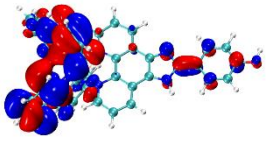
LUMO+7	**LUMO+6**	**LUMO+5**
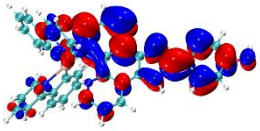		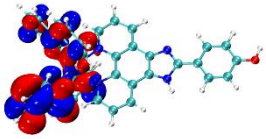
LUMO+4	**LUMO+3**	**LUMO+2**

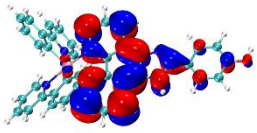	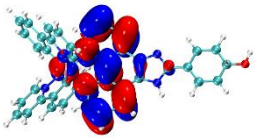	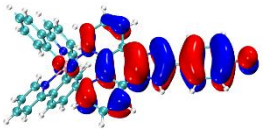
LUMO+1	**LUMO**	**HOMO**
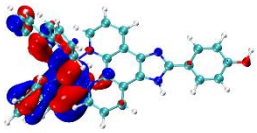	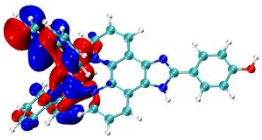	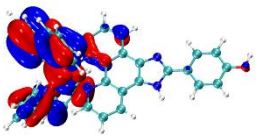
HOMO–1	**HOMO–2**	**HOMO–3**
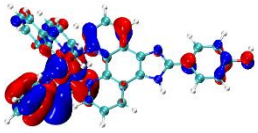	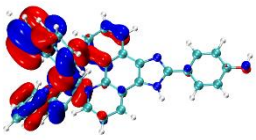	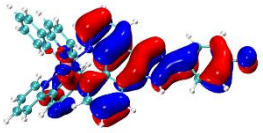
HOMO–4	**HOMO–5**	**HOMO–6**
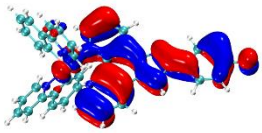	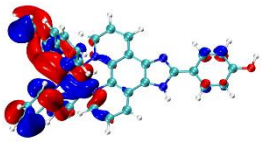	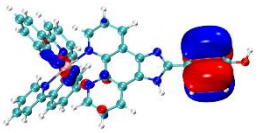
HOMO–7	**HOMO–8**	**HOMO–9**
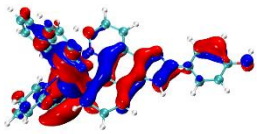		
HOMO–10		

Table S14. Molecular Orbital Compositions of **IrLH** under TD-DFT Triplet Excitation Calculation (Emission Transition Study).

Orbital	Energy(eV)	MO contribution (%)		
		Ir	ppy	L
LUMO+10	-0.0892	6.51	84.81	8.65
LUMO+9	-0.6057	1.33	2.66	95.99
LUMO+8	-0.9924	0.02	0.03	99.94

LUMO+7	-1.0941	1.82	31.35	66.82
LUMO+6	-1.1595	1.27	83.82	14.91
LUMO+5	-1.4053	1.22	82.45	16.33
LUMO+4	-1.7639	3.67	95.21	1.12
LUMO+3	-1.8274	3.60	94.38	2.01
LUMO+2	-2.3767	0.67	1.00	98.31
LUMO+1	-2.5905	1.22	1.30	97.46
LUMO	-3.1873	4.62	2.76	92.60
HOMO	-6.0845	30.58	62.57	6.85
HOMO–1	-6.5499	24.69	72.15	3.15
HOMO–2	-6.9904	15.41	26.96	57.63
HOMO–3	-7.0047	3.92	75.88	20.20
HOMO–4	-7.1073	3.89	83.26	12.84
HOMO–5	-7.2626	47.67	24.04	28.29
HOMO–6	-7.8546	23.20	66.84	9.97
HOMO–7	-8.0115	15.23	36.20	48.56
HOMO–8	-8.1563	21.52	66.60	11.90
HOMO–9	-8.1919	6.69	16.45	76.84
HOMO–10	-8.2259	0.62	1.10	98.27

Table S15. TD-DFT Excitation Calculation for Emission for **IrLH**.

State	Transition	Contribution%	*E*,nm (eV)	o.s.	Assignment
T1	HOMO→LUMO	92.0	670 (1.85)	0.0000	^{3}MLCT//^{3}LLCT
T2	HOMO–1→LUMO	31.9	508 (2.44)	0.0000	^{3}MLCT/^{3}LLCT
T3	HOMO–1→LUMO	60.8	501 (2.48)	0.0000	^{3}MLCT/^{3}LLCT
T4	HOMO→LUMO+1	64.8	474 (2.61)	0.0000	^{3}MLCT/^{3}LLCT
T5	HOMO→LUMO+3	54.4	457 (2.72)	0.0000	^{3}MLCT
T6	HOMO–2→LUMO	21.6	441 (2.81)	0.0000	^{3}MLCT/^{3}LLCT
T7	HOMO–1→LUMO+4	36.1	429 (2.89)	0.0000	^{3}MLCT
T8	HOMO–2→LUMO+2	30.2	421 (2.94)	0.0000	^{3}MLCT/^{3}LLCT
T9	HOMO–3→LUMO	32.6	404 (3.07)	0.0000	^{3}LLCT ^{3}ILCT

Table S16. Calculated molecular orbitals of **IrLH** under excited states TD-DFT (Emission Transition).

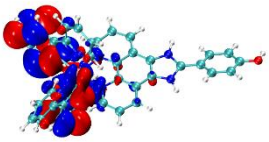	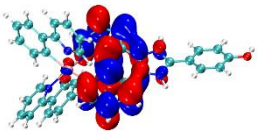	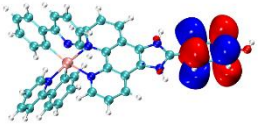
LUMO+10	**LUMO+9**	**LUMO+8**
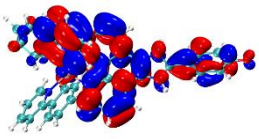	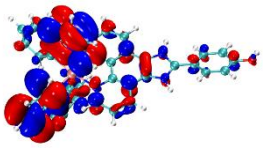	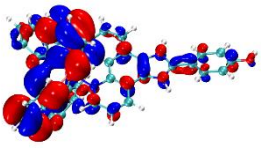
LUMO+7	**LUMO+6**	**LUMO+5**

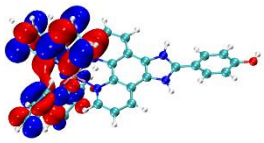	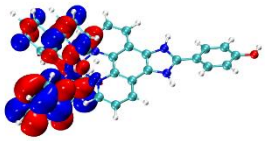	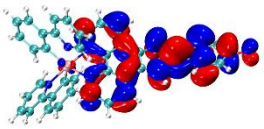
LUMO+4	**LUMO+3**	**LUMO+2**
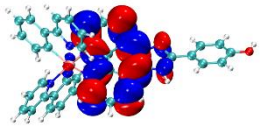	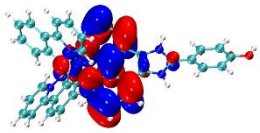	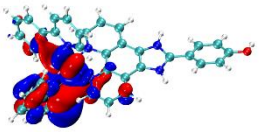
LUMO+1	**LUMO**	**HOMO**
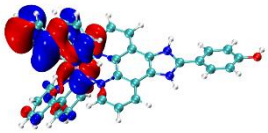	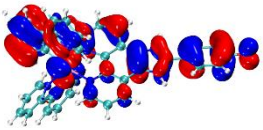	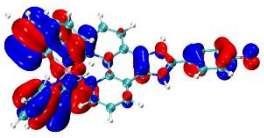
HOMO–1	**HOMO–2**	**HOMO–3**
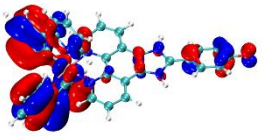	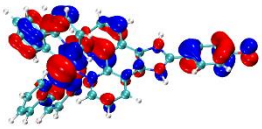	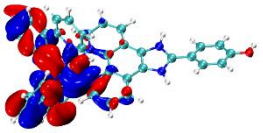
HOMO–4	**HOMO–5**	**HOMO–6**
	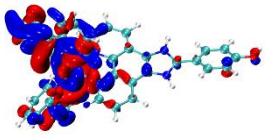	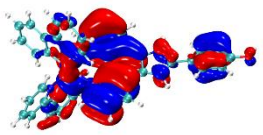
HOMO–7	**HOMO–8**	**HOMO–9**
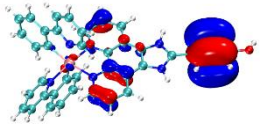		
HOMO–10		

Table S17. TD-DFT Calculation for the Triplet Transition and MO Contribution of **IrL** and **IrLH** in Acetonitrile.

Complex	State	Transition	Contribution%	E/nm (eV)	Assignment
IrL	T1	HOMO→LUMO	82.5	586 (2.12)	^{3}ILCT
IrLH	T1	HOMO→LUMO	92.0	670 (1.85)	^{3}MLCT/^{3}LLCT

Table S18. Single oxygen generation was determined using UV-vis spectroscopy under various experimental conditions.

Entry		Complex (μM)	ABDA (μM)	Light (nm)	Time (min)	Ar	NaN_3 (mM)	k (min^{-1})
1	**IrL**	10	100	390	1/10	-	-	0.2653
2	**IrL**	10	100	390	1/10	yes	-	0.0222
3	**IrL**	10	100	390	1/10	-	10	0.1478
4	$[Ru(bpy)_3]Cl_2$	10	100	390	1/10	-	-	0.1909

Table S19. Photocatalytic oxidation of NADH by **IrL** in deionized water under various conditions.

Entry		Complex (μM)	NADH(μM)	Light (nm)	Time (min)	Ar	k (min^{-1})
1	**IrL**	10	100	390	1/10	-	0.0900
2	**IrL**	10	100	390	1/10	yes	0.0377
3	$[Ru(bpy)_3]Cl_2$	10	100	390	1/10	-	0.0372
4	-	-	100	390	1/10	-	0.0031

Table S20. Single oxygen generation under three different pH conditions.

Entry	pH	IrL (μM)	ABDA(μM)	Light (nm)	Time (min)	k (min^{-1})
1	7.4	10	100	390	1/10	0.1238
2	6.5	10	100	390	1/10	0.1414
3	4.5	10	100	390	1/10	0.2597

Table S21. Photocatalytic oxidation of NADH by **IrL** in PBS buffer with different pH.

Entry	pH	IrL (μM)	NADH(μM)	Light (nm)	Time (min)	k (min^{-1})
1	7.4	10	100	390	1/10	0.0342
2	6.5	10	100	390	1/10	0.0523
3	4.5	10	100	390	1/10	0.1075

Table S22. IC_{50} values of **IrL** against different cell lines under normoxic and hypoxic conditions after incubation for 48 h.

IC_{50} (μM), IrL						
	Normoxia (21% O_2)			**Hypoxia (5% O_2)**		
	Dark[a]	**Light**[b]	**phototoxicity index** [c]	**Dark**[a]	**Light**[b]	**phototoxicity index** [c]
4T1	83.8	2.0	41.9	51.6	6.6	7.8
EMT6	76.1	0.6	126.8	40.6	1.2	33.8

[a] Cells were treated with the **IrL** for 48 h. [b] Cells were treated with the **I IrL** for 4 h before irradiation.
[c] phototoxicity index = IC_{50}(dark)/IC_{50}(light).